UNIVERSITY OF CALGARY

# Feasibility Analysis on Geothermal Heat Storage Capacity and Recovery of Alberta's Decommissioned Wells

By

Sarvenaz Moazami

A RESEARCH PROJECT SUBMITTED

IN PARTIAL FULFILMENT OF THE REQUIREMENTS FOR THE

DEGREE OF MASTER OF SCIENCE

GRADUATE PROGRAM IN SUSTAINABLE ENERGY DEVELOPMENT

CALGARY, ALBERTA

AUGUST 2020

**Abstract**

The province of Alberta is home to one of the World's largest strategic sedimentary basins. The Oil and Gas industry has been Alberta's major source of economic prosperity for more than half a century. There are plenty of related environmental concerns with the oil and gas operations. The Earth's thermal energy potential known as Geothermal is one the most reliable sustainable energy sources with the least negative environmental impacts. In this capstone project, a feasibility analysis with numerical model was performed for heat storage and recovery, to create synthetic geothermal reservoirs in Alberta's cold shallow formations. Additionally, an analytical model was created to recover sustainable heat for space heating applications from hot deep deposited formations using the decommissioned wells. The objective of this study is to provide a sustainable solution to meet some of the Alberta's growing energy mix demand for the future while lowering the GHG emissions and negative environmental impacts of the abandoned oil and gas wells.

**Acknowledgement**

I would like to thank the University of Calgary and Sustainable Energy Development Program. I am grateful to my supervisor, Dr. Roman Shor, and his guidance, time, and help. I owe a sincere gratitude to my former colleagues at Schlumberger Dr. Jose Rivero, Dr. Robert Stacey, Majid Faskhoodi and Christopher Istchenko for their help, and willingness to share their expertise. I would like to thank my friend Dr. Sanaz Saeid from DELF University for her advice and knowledge share.

**Table of Contents**

**List of Tables**

**List of Figures**

**Chapter 1: Introduction**

The province of Alberta is home to one of the World's largest strategic sedimentary basins. The Oil and Gas industry has been Alberta's major source of economic prosperity for more than half a century (Figure 1). The oil sand deposits are the province's biggest oil producers, and due to the nature of bitumen and heavy crude oil residing in these basins, enhanced oil recovery techniques such as SAGD (Steam-Assisted Gravity Drainage) and VAPEX (Vapor Extraction) are required for heavy oil extraction.

*Figure 1: Western Canada Sedimentary Basin*


*(Packer Plus, 2020)*

In SAGD advanced steam stimulation method, two horizontal wells are drilled, high-pressure steam is being continuously injected in the upper injector well, to heat the bitumen and decrease its viscosity with time to be drained and produced from the lower production well. In VAPEX process, high temperature vaporized hydrocarbon solvent is injected into bitumen reservoirs, the solvent-diluted oil drains into a horizontal production well. Both technologies consume high amount of natural gas energy to produce steam or vaporize the solvents (Figure 2).

In addition to huge oil sands, heavy oil, the conventional and unconventional oil and gas productions in Alberta, there are some decommissioned oil and gas fields with close proximity to residential areas, where hydrocarbon was being produced from formations deposited deeper underground with high bottom hole temperature. The abandoned wells in these fields are huge liabilities to companies and government causing human health concerns. Recently these issues have made growing concerns about the environmental impacts of the oil and gas operations, and the non-sustainability nature of fossil fuels resources.

*Figure 2: Steam Assisted Gravity Drainage*

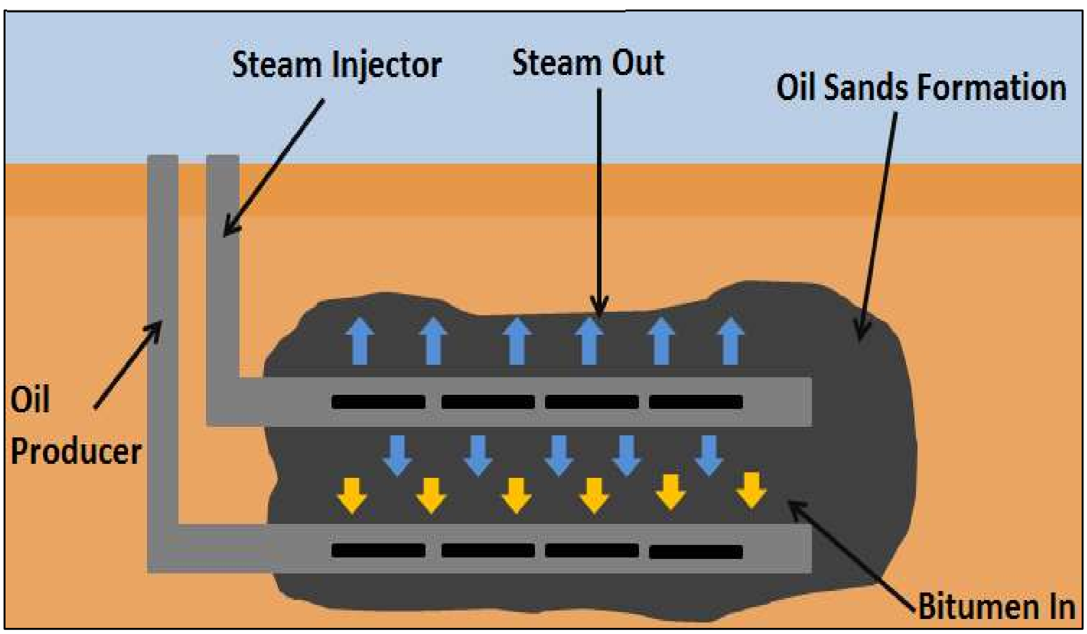


*(J.M.K.C. Donev, 2018)*

The Alberta Grid ranks the highest GHG emitter among provinces and territories across Canada (Figure 3). The concerns around negative environmental impacts, and the risk and liabilities of the oil and gas decommissioned wells, emphasize on the necessity for much cleaner solutions to meet Alberta's future energy demand.

*Figure 3: Provincial GHG Emissions by Energy Source*

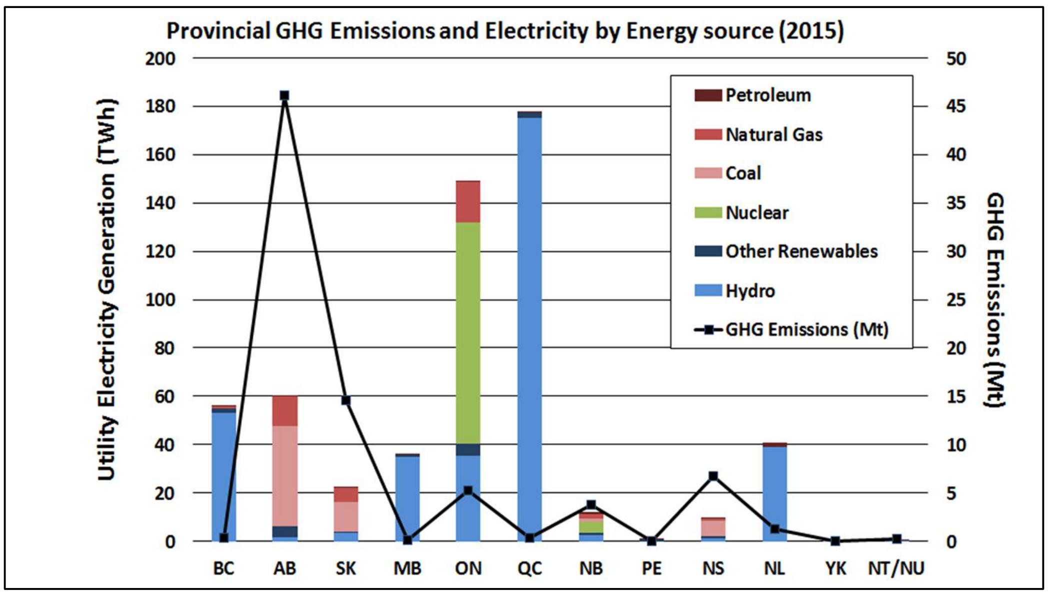


*(Hislop, 2018)*

Geothermal is one of the most reliable and sustainable natural resources with little environmental impacts which can be exploited for power generation and space heating applications. The geothermal heat generation potential of subsurface reservoirs depends on several factors such as thermal gradient, depth of deposition, reservoir capacity and heat recovery. Although, not all the sedimentary basins around the world are blessed with the geothermal potential to generate natural high heat for steam generation, the subsurface reservoir formations could be used as a medium for thermal energy storage, known as GeoTES (Wendt, 2019). By creating such synthetic geothermal reservoirs, the wasted heat from surface can be stored and recovered when required to generate electricity power. This approach will create a sustainable energy storage backup for other weather dependant renewable sources, therefore higher penetration to electric grid by renewable energies and lower negative environmental impacts associated with fossil fuels are achievable.

In this Capstone project, the heat storage capacity of shallow cold formations with low borehole temperature has been evaluated, such as abandoned oil sands pads post SAGD operations. These systems have been assessed using reservoir simulation to evaluate the multiple factors affecting the heat storage capacity and recovery efficiency for geothermal heat storage. In this study, the heat recovery potential of natural warmer formations that exist due to deeper depth of deposition, has also been researched. The heat recovery potential of these formations has been assessed for nearby residential heating applications from the existing decommissioned wells (Figure 4).

*Figure 4: Heat Recovery from Hot formations*

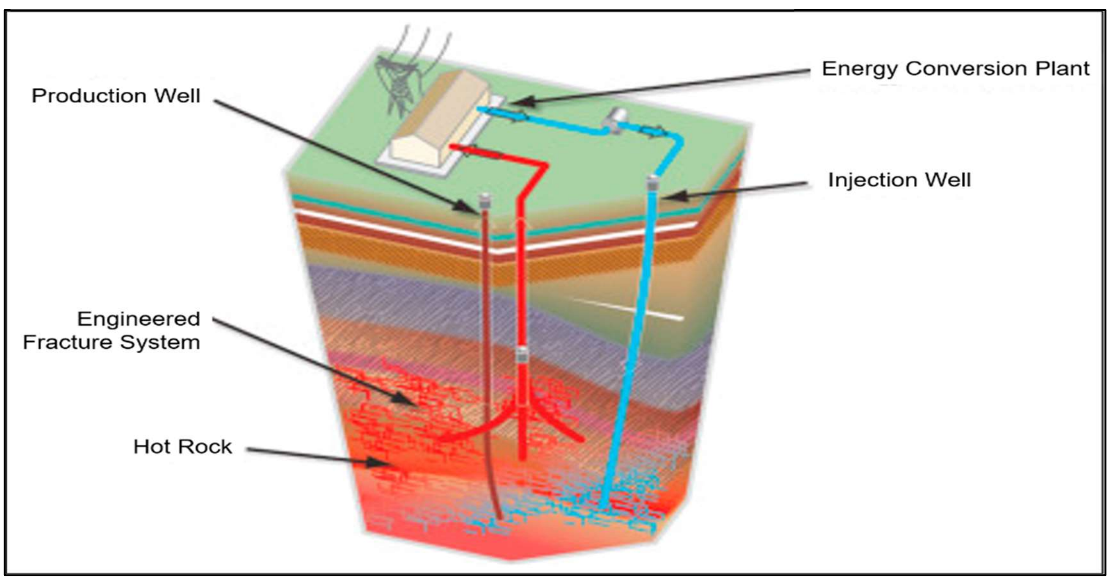


*(Hirschmiller, 2019)*

### 1.1. Research Questions

In this capstone project, the following research questions have been worked on: "How thermal energy can be stored and recovered from shallow cold deposited formations, where borehole temperature is naturally low, in other words creating synthetic geothermal energy storage (GeoTES) by injecting and storing steam into depleted SAGD Pads. And, how natural heat from deeper hotter sediments with higher borehole temperature can be recovered from decommissioned wells and utilized for residential heating applications". To achieve the results presented in this report, analytical models were created, for feasibility analysis using data from two different locations.

FIREBAG oil Sand operation is one of the world's largest in situ operations located 120km northeast of Fort McMurray, data from FIREBAG SAGD Pads' end of life were used for creating GeoTES model. The idea was to create a 100% sustainable reliable micro grid, to collect heat from parabolic solar trough heat collectors, generate steam for electricity and then inject the excess steam into these depleted pads acting as storage to be recovered when solar radiation is not available for electricity generation.

Turner Valley is an old oilfield in the Calgary Region, within the Municipal District of Foothills, data from old decommissioned wells from this field was used to do feasibility analysis for space heating applications for the nearby residential areas.

## 1.2. Interdisciplinary Aspects

This feasibility study is an interdisciplinary research, addressing environmental, energy and economic dimensions of the Geothermal potential in Alberta. The implications of this study within these disciplines are summarized as:

### 1.2.1. Energy

In this project, Earth's heat energy storage and recovery potential has been studied for electricity generation and residential areas heating applications. This provides a sustainable solution to meet Alberta's growing energy demand for future, and alternative clean energy solution for remote areas in the province.

### 1.2.2. Environment

The objective of this study is to provide a sustainable solution for energy demand while lowering the GHG emissions by replacing fossil fuels with renewable sources with the least negative environmental impacts and decreasing the health and pollution risks regarding abandoned oil and gas wells.

### 1.2.3. Economics

The initial investment needed for converting existing oil and gas infrastructure into Geothermal energy generation, and the projects' total revenue and costs have been analyzed in this report. This provides an insight into economical viability of such projects with this approach for the potential project owners and investors.

## Chapter 2: Literature Review

Geothermal energy relies on heat from the Earth. This energy is combination of the residual heat from subsurface formations, combined with the radioactive decay of the subsurface isotopes (Reid, 2017). These two mechanisms result in geothermal heat that increases with the depth. Heat is transferred via three mechanisms:

- Radiation is heat transfer by the emission and absorption of thermal photons.
- Conduction is the transfer of energy between atoms of a material.
- Convection is the movement of warm mass towards a cooler region.

Normally subsurface fluid travels slow and lose heat energy to surrounding rocks, if rising quickly to surface before complete heat transfer, hot springs or geysers can take place. The Earth thermal heat can be harnessed for clean electricity generation, however, for electricity generation high or medium temperature resources are needed, which are usually located close to tectonically active regions, such as California, El Salvador, New Zealand, Indonesia, and the Philippines. In other scenarios, where the geothermal heat is not high enough for electricity generation, it can be utilized for space heating applications.

There are several publications and related studies performed on geothermal potential in Alberta (Hirschmiller, 2019). In this study focus has been on two master's degree projects submitted for University of Calgary. One had studied the Alberta SAGD reservoirs residual geothermal heat potential for electricity generation (Omusi, 2019), and the other one had focused on Alberta's decommissioned wells geothermal potential for district heating applications (Reid, 2017).

In addition, there are similar studies and projects for heat storage and recovery being done in other countries such as United States (Augustine, 2014). Those reports have been reviewed and determined how to implement their findings in this capstone project. There are different parameters to account for, based on different locations and geology, which are tried to be implemented in this study by having some local knowledge on Alberta's oil and gas operations.

The literature review has been conducted, on the existing natural geothermal reservoirs and considered how much thermal energy is needed for a certain amount of power generation (Budd, 1984). Then compared that number to depleted SAGD PADS and performed a feasibility analysis, to see if electricity generation would be technically and economically viable, by converting SAGD pairs into heat injection and recovery for geothermal operations.

For the surface facilities and boundary considerations, the literatures related to parabolic solar heat trough collectors have been reviewed (Quaschning, 2003), the number and design of the solar heat troughs to heat up the fluid to generate steam, to be injected in the formations has been evaluated (McTigue, 2018). A study done in Kuwait for renewable energy production from solar heat collectors, provided valuable information and parameters for this study microgrid surface facility assumptions (Nayef, 2013).

The publications related to natural hot reservoirs, where the heat has been used for nearby residential heating applications (Lee, 2013) have been reviewed, and compared to similar reservoirs in Alberta. There was a great study done for SEDV program in 2017 for Geothermal district heating applications (Reid, 2017), the findings in that report and limitations to consider in the similar case proposed in this feasibility analysis has been used.

## 2.1. Geothermal Heat Storage

In the previous study done on Alberta SAGD reservoirs geothermal potential (Omusi, 2019), the residual heat preserved underground from SAGD steam injection has been analyzed to be recovered to produce steam for Organic Rankine Cycle (ORC) electricity generation, backed by a gas turbine. In this study, a 100% sustainable microgrid is being proposed to meet a 1000 households electricity demand nearby FIREBAG SAGD operation. To achieve this, parabolic solar heat troughs are designed for enough heat collection when solar radiation is available for steam production during daytime. The steam is then utilized for electricity generation and the excess steam to be injected into the depleted SAGD pads acting as geothermal storage and be recovered during nighttime or times when solar radiation is not available.

## 2.2. Geothermal District Heating

The study on Geothermal Heat in Calgary, performed for SEDV program (Reid, 2017) had done a reasonable analysis on the Alberta wells geothermal potential. In that study, the numerical analysis for heat transfer from the subsurface and heat pump are proposed. Turner Valley location data have been selected. Turner Valley is an old gas field in the Calgary Region, within the Municipal District of Foothills, the proximity of this field to residential area makes it a good candidate for district heating applications. A geothermal district heating for 1000 households is being proposed. Assuming the buildings are having good insulation and proper construction codes, where building temperature can be warmed up from -15 C° (outside cold air) to 25 C° by geothermal heat pumps.

**Chapter 3: Methodology**

The first step performed for this capstone project was choosing two best locations in Alberta to design for:

- End of life SAGD PADS, where originally formations are shallow, ideal for geothermal heat storage
- Deeper decommissioned wells from an old oil or gas field operation with proximity to residential area, where formations are deep and warm, ideal for geothermal space heating application

For this purpose, IHS Markit (ihsmarkit, 2020) AccuMap publicly available data has been used. Then numerical models have been created by having subsurface and surface data to come up with results for geothermal heat storage and geothermal residential space heating. These results with the public available data from oil and gas operations have been compared, to see if the results are reasonable and practical given the size of surface facilities and subsurface network of wells needed.

The idea for this capstone project was how to utilize Alberta decommissioned wells geothermal potential, for thermal heat storage or district heating. For this, a model was designed to provide a community of 1000 households electricity demand by a 100% renewable microgrid and geothermal heat storage proposed as the backup, where GHG emissions is eliminated to almost zero, which is explained in detail in chapter 4. For district space heating, an analysis for heat energy needed for a 1000 households community heating needs has been performed.

The average electricity consumption for a typical household in Alberta, is about 7,000 kWh annually. It has been assumed that in base scenario, natural gas is burnt for steam and then electricity generation. For this project, the electricity demand has been replaced with 100% solar heat microgrid with power of 1 MW, backed up by a geothermal heat storage. The parabolic solar heat collectors are designed to collect enough heat during day for steam generation to produce electricity and the excess steam to be injected and stored into depleted SAGD pairs, and only be recovered at night for 6 hours when solar radiation is not available and generate electricity from this geothermal heat storage.

For residential space heating, the data for Alberta's average single family building square footage and volume of air needed to be displaced in the coldest month of the year has been analyzed. It has been designed for heat pumps to use R134a refrigerant to warm an average building up to 25 C° from average cold temperature of -15 C°. Then the results were checked with the decommissioned wells data and the amount of thermal heat to be recovered from those wells to warm up a community of 1000 households. Based on these two assumptions, the number of wells and flow rate needed to provide the amount of 5 MW heat power capacity for the community of this size, have been concluded

### 3.1. Geothermal Heat Storage using SAGD PADS

Canadians are concerned with their high amount of GHG emissions per capita and are looking for solutions to lower their carbon footprints. In 2014, the average Canadian household used 11,135 kWh of electricity per year. The average household in Alberta uses about 7,000 kWh per year, this lower offset compared to the nationwide consumption is due to higher usage of natural gas. Most of the renewable energy sources such as solar and wind are highly intermittent and weather dependant. To have a sustainable stable grid, which is not interrupted by weather or seasonal intermittency, a reliable energy storage or battery is essential to back these sources. The electrochemical batteries are quite expensive and need continuous maintenance with high replacement costs.

In this capstone project, the problem has been investigated by proposing a solution of a 100% renewable microgrid to provide sustainable reliable electricity for a community of 1000 households. A network of parabolic solar trough heat collectors has been designed, to provide enough heat to generate steam and electricity during day light, when solar radiation is available and then the excess steam to be injected into depleted SAGD pads to be recovered for a duration of 6 hours at night time when sunlight is absent (Figure 5).

After analyzing the data and several SAGD operations across Alberta, I have selected the FIREBAG post SAGD operation pads to be converted into synthetic geothermal storage (GeoTES). FIREBAG oil sand operation is one of the world's largest in situ operations located 120km northeast of Fort McMurray (Figure 6).

*Figure 5: 100% Microgrid design with geothermal heat storage*

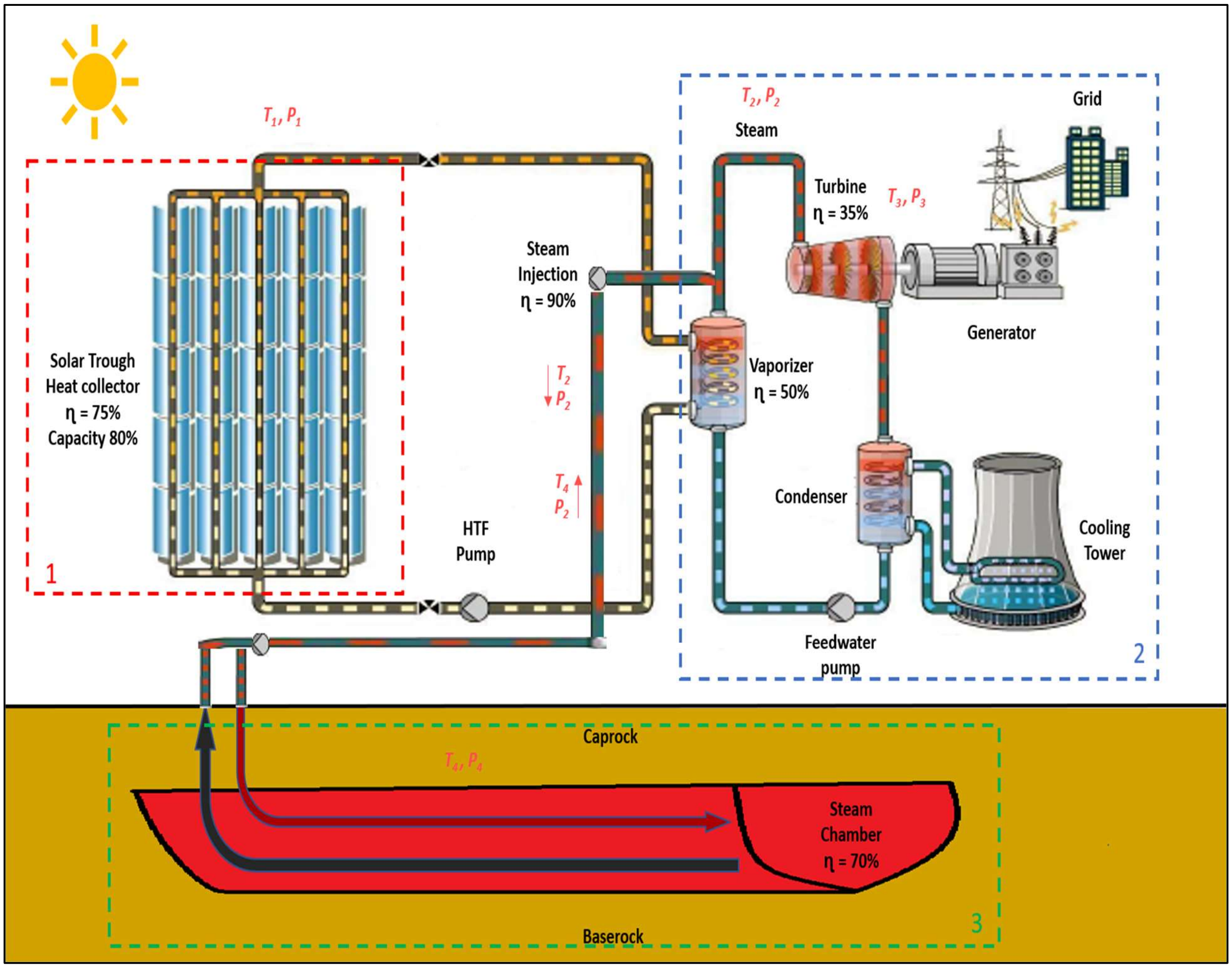


(Moazami, 2020)

As shown in Figure 5, for a 100% renewable microgrid design, It has been accounted for:

- Selection 1: Parabolic solar heat trough collectors, for heat source
- Selection 2: The conventional Rankine Cycle for steam and electricity generation
- Selection 3: The geothermal heat storage by injecting steam into SAGD depleted PADS

*Figure 6: FIREBAG Oil Sand Operations Location*

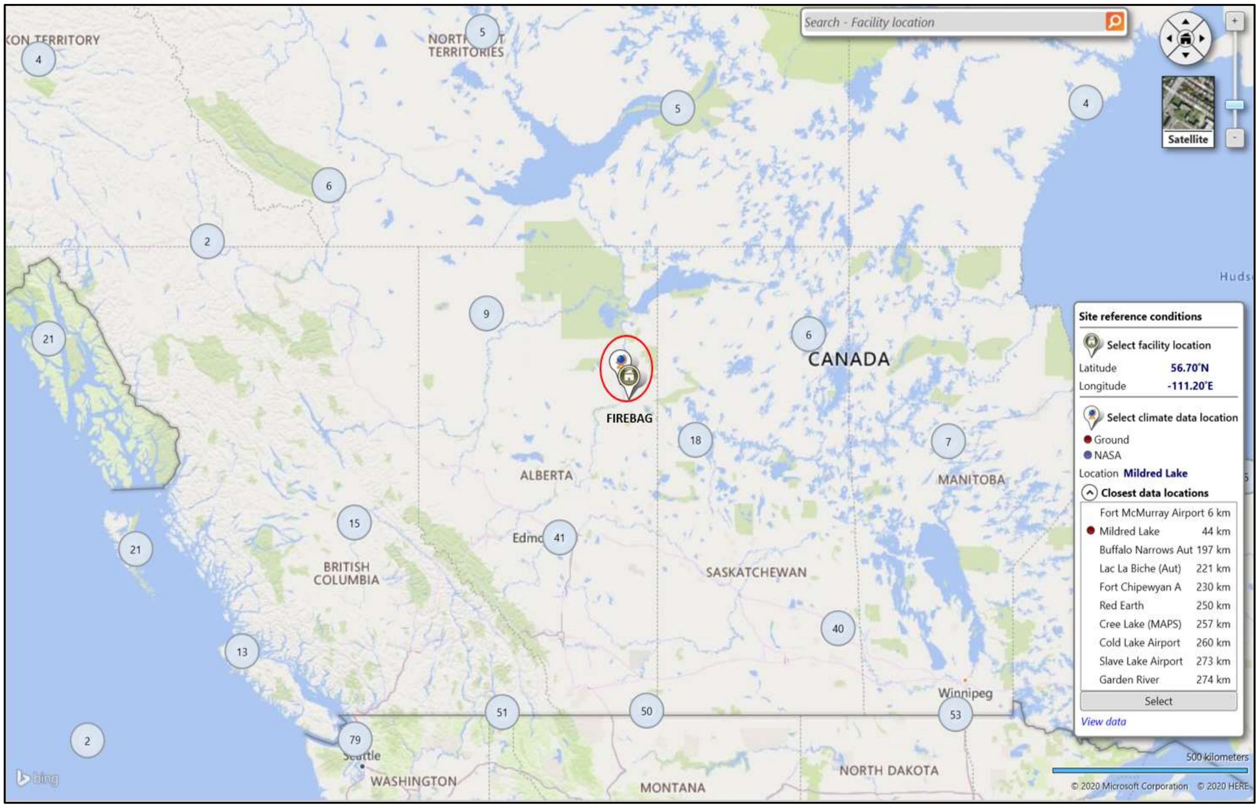


*(RetScreen, 2020)*

A geothermal system has three main elements, a reservoir, heat source and a carrier fluid. In natural geothermal reservoirs, the heat source is a combination of formation residual heat and radioactive decay of subsurface isotopes. The sedimentary geologic reservoirs can act as a medium for thermal energy storage (TES), the caprock and base rock formations confining the reservoir rock have significantly lower permeabilities than the reservoir, making it ideal conditions for the heat to be stored with little heat loss. Therefore, a synthetic Geothermal storage (GeoTES) system can be designed in shallow cold formations, by accounting for, Heat Input, Storage, Recovery and Heat to electric conversion. All these have been considered and designed for this study's geothermal storage.

*Figure 7: FIREBAG Location, Solar radiation, and Weather data*

| Month | Air temperature | Relative humidity | Precipitation | Daily solar radiation - horizontal | Atmospheric pressure | Wind speed | Earth temperature | Heating degree-days 18 °C | Cooling degree-days 10 °C |
|---|---|---|---|---|---|---|---|---|---|
| | °C | % | mm | kWh/m²/d | kPa | m/s | °C | °C-d | °C-d |
| January | -17.7 | 79.8% | 24.18 | 0.58 | 96.1 | 2.5 | -20.8 | 1,107 | 0 |
| February | -12.3 | 77.3% | 19.60 | 1.44 | 96.2 | 2.6 | -16.6 | 848 | 0 |
| March | -6.2 | 66.8% | 29.45 | 2.92 | 96.2 | 3.1 | -9.9 | 750 | 0 |
| April | 3.8 | 56.0% | 35.40 | 4.59 | 96.2 | 3.5 | 0.9 | 426 | 0 |
| May | 10.2 | 58.4% | 58.28 | 5.48 | 96.1 | 3.4 | 8.6 | 242 | 6 |
| June | 15.9 | 63.5% | 84.90 | 5.68 | 95.9 | 3.2 | 14.1 | 63 | 177 |
| July | 18.2 | 68.4% | 73.47 | 5.55 | 96.0 | 3.1 | 16.7 | 0 | 254 |
| August | 16.4 | 71.3% | 58.59 | 4.59 | 96.0 | 3.0 | 15.1 | 50 | 198 |
| September | 10.8 | 73.4% | 51.90 | 3.06 | 96.0 | 3.2 | 8.7 | 216 | 24 |
| October | 3.0 | 75.5% | 36.58 | 1.67 | 96.0 | 3.2 | 0.5 | 465 | 0 |
| November | -6.9 | 82.4% | 28.50 | 0.80 | 95.9 | 2.8 | -10.7 | 747 | 0 |
| December | -13.5 | 82.7% | 23.25 | 0.36 | 96.0 | 2.6 | -18.7 | 977 | 0 |
| **Annual** | **1.9** | **71.3%** | **524.10** | **3.07** | **96.1** | **3.0** | **-0.9** | **5,890** | **660** |
| **Source** | Ground | Ground | NASA | NASA | NASA | Ground | NASA | Ground | Ground |
| Measured at | | | | | m | 10 | 0 | | |

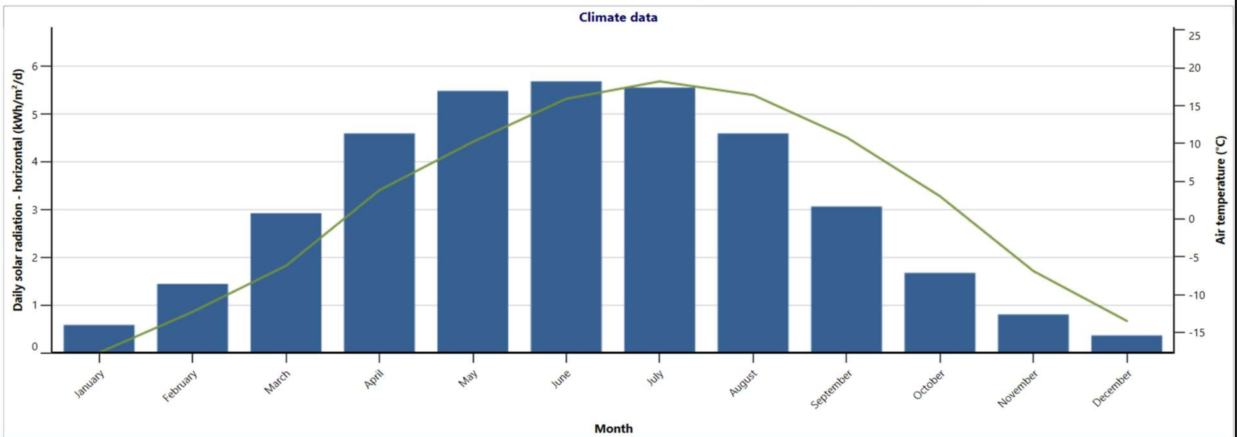


*(RetScreen, 2020)*

The solar radiation availability and weather data for FIREBAG location, has been provided from RetScreen in Figure 7. The data is monthly average information. These data have been used for this project microgrid design, and the number of solar troughs to account for this location and this size of the project. All the calculations and designs are based on the month of December; the number of solar troughs needed for this month with the lowest solar radiation availability would be sufficient for other months to meet the demand.

### 3.1.1. Heat source, Parabolic Solar Trough

Parabolic solar trough heat collectors, are made of large curved mirrors, the parabolic shape concentrates the sunlight by almost 80% to a focal line (Figure 8). The focal line is made of a metal absorber tube, which is inside an evacuated glass tube and is coated additionally with a special high-temperature resistive material, designed to minimize the heat losses. The parallel collectors' rows are built up of multiple collectors, 300-600 meters long. Each trough consists of 8 sections and in total an area of about 50 $m^2$ (Soucy, 2014), operating at 75% efficiency and 80% capacity. The design allows the solar collector to track sun from East to West.

*Figure 8: Parabolic Solar Trough*

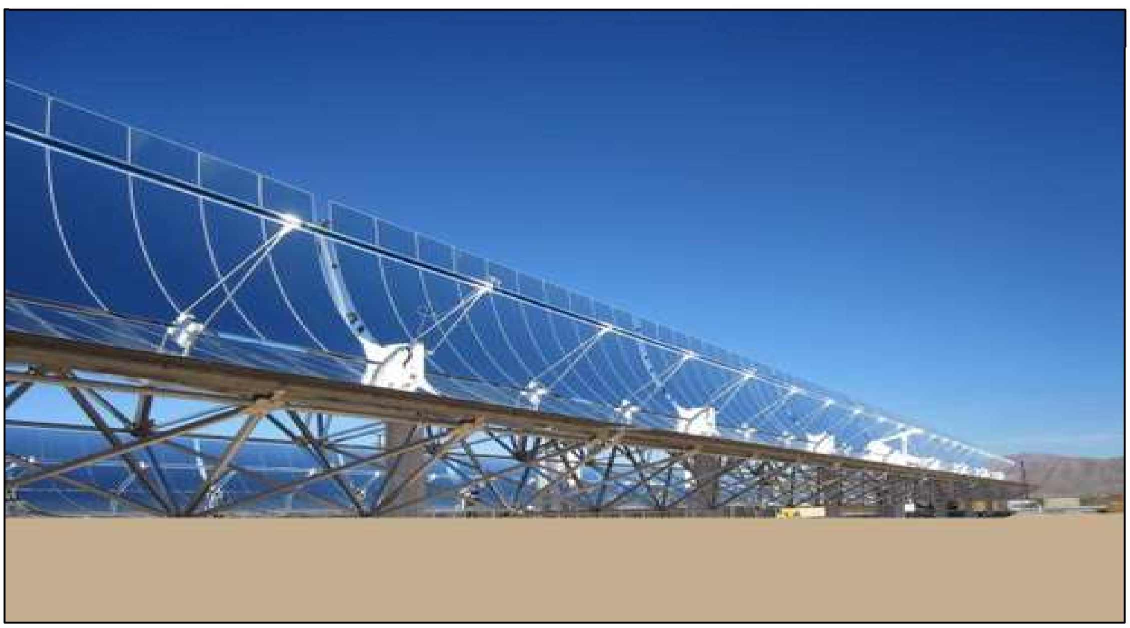

*(Zipp, 2012)*

The one-axis tube can heat up the heat transfer fluid (HTF) passing through the tube up to nearly 400 °C, and then transfer the heat to the Rankine cycle. The heat can boil water to make steam for electricity generation and geothermal storage.

The solar thermal power plants can guarantee the capacity to generate enough heat for steam production during daytime and excess amount for storage to be utilized during the nighttime or when the weather is bad (Figure 9). With geothermal storage, the plant can generate electricity even when there is no solar radiation available.

*Figure 9: Solar thermal power plant with storage*

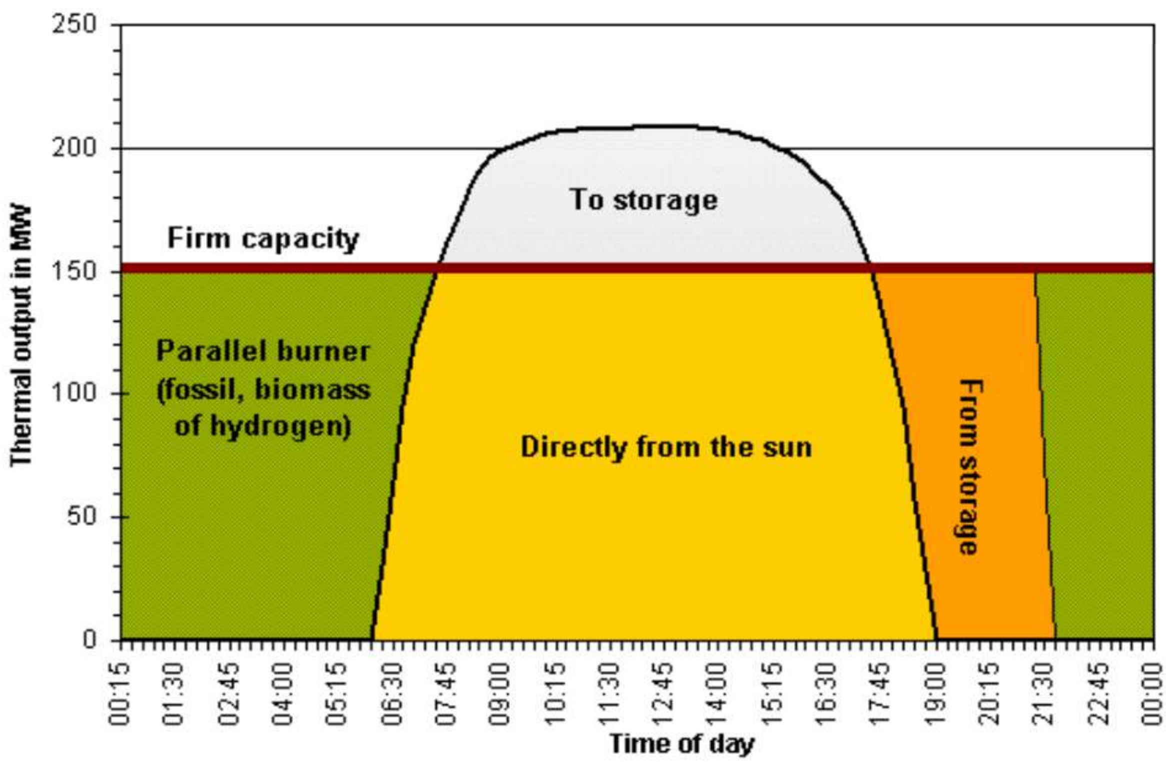


*(Quaschning, 2003)*

### 3.1.2. Rankine Cycle

Rankine cycle is a model to monitor the steam turbine performance. Rankine cycle is a thermodynamic cycle of heat engine, consisting of pump, boiler, turbine, and condenser (Selection 2, Figure 5). The feedwater pump pressurizes the water and then boiler/vaporizer produces superheated steam. The steam turbine is connected to electrical generator which converts mechanical energy into electrical energy. The condenser condenses the steam into water, which goes through feedwater pump and closes the cycle.

### 3.1.3. Geothermal heat storage

The subsurface sedimentary reservoirs can be used for heat/steam storage. A reservoir is a porous medium, where fluid (hydrocarbon) can be stored and due to connectivity of the pores the fluid can be mobilized within the reservoir, known as permeability. The reservoir rock should be confined with impermeable formations, base rock on the bottom and cap rock on the top, to make sure fluid is kept and trapped. In oil and gas operations, wells are drilled into these reservoirs to extract the hydrocarbon.

In SAGD advanced steam stimulation method, two horizontal wells are drilled, high-pressure steam is being continuously injected in the upper injector well, to heat the bitumen and decrease its viscosity with time to be drained and produced from the lower production well. The two wells combination is referred to as SAGD pairs. In Alberta's SAGD operation, the norm is to drill a combination of 12 pairs in a pad.

Depleted SAGD pads are ideal candidates for steam storage. The sedimentary reservoir, the porous medium with confining base and cap rocks do exist. The wellbores or the pairs are already drilled, otherwise, drilling cost being significantly high could be a big portion of the initial cost to account for. The wells were designed from the beginning for high temperature/pressure steam injection. The depleted section of the reservoir's residual temperature remains extremely high post SAGD operation for quite some time. SAGD pairs are shallow and easy to inject and recover steam when needed.

### 3.1.4. Model for 100% Renewable Microgrid with Geothermal storage as backup

The numerical model for the 100% renewable microgrid with geothermal storage to generate electricity for 1000 households (Appendix A) has been modelled. The average household electricity demand is 7,000 kWh per year, the consumption is changing for different months of the year. The calculations were done based on different months. The number of solar troughs was set based on month of December the coldest month of the year with least amount of available solar radiation ( Table 1).

FIREBAG is located at 57.24° N Latitude and 110.89° W Longitude. The monthly available solar radiation data for this location is given in Table 1 (RetScreen, 2020). The monthly electricity consumption was assumed per households and then determined for 1000 households daily demand. This would be the amount of electricity the microgrid has to output from the generator and transfer through the grid.

Reasonable efficiencies for different parts of the microgrid process and the geothermal storage have been assumed:

- Parabolic Solar Trough Heat collector: Efficiency 75%, Capacity 80%
- Vaporizer: Efficiency 50%
- Steam Turbine: Efficiency 35%
- Steam Injection pipes: Efficiency 100%
- Steam Storage: Efficiency 70%, Steam Quality 85%

*Table 1: FIREBAG Location, Solar Radiation, and average energy consumption data*

| Month | Surface Temperature | Daily Solar Radiation Power | Atmospheric Pressure | Average Electricity consumption per household a month | Average Electricity consumption for 1000 household a month | Average Electricity for 1000 household per day |
|---|---|---|---|---|---|---|
| | C° | kWh/m2/d | kPa | kWh | kWh | kWh/day |
| January | -9.6 | 1.58 | 100.9 | 800 | 800000 | 26666.67 |
| February | -7.8 | 2.53 | 100.9 | 800 | 800000 | 26666.67 |
| March | -2.3 | 3.62 | 100.9 | 800 | 800000 | 26666.67 |
| April | 5.6 | 4.46 | 100.7 | 500 | 500000 | 16666.67 |
| May | 13.4 | 5.1 | 100.7 | 400 | 400000 | 13333.33 |
| June | 18.9 | 5.61 | 100.5 | 400 | 400000 | 13333.33 |
| July | 20.5 | 5.52 | 100.6 | 400 | 400000 | 13333.33 |
| August | 19.5 | 4.91 | 100.7 | 400 | 400000 | 13333.33 |
| September | 15.1 | 3.77 | 100.9 | 400 | 400000 | 13333.33 |
| October | 8.3 | 2.38 | 100.9 | 500 | 500000 | 16666.67 |
| November | 2.1 | 1.45 | 100.9 | 800 | 800000 | 26666.67 |
| December | -4.5 | 1.28 | 100.9 | 800 | 800000 | 26666.67 |

*(Moazami, 2020)*

The steps have been explained of how to get the correct number of solar troughs and the amount of steam to be injected underground to be recovered at nighttime when solar radiation is not available. The microgrid was designed based on the calculations needed to fulfill demand in December which can be sufficient for the rest of the year, the average daily electrical energy needed in December is calculated in Table 1.

The amount of energy to be output from turbine to generator for electricity generation is:

Input Energy to Turbine = Output Generated Electricity / Turbine efficiency

Input Energy to Turbine = Output Generated Electricity / 0.35

The amount of energy to be output from vaporizer to be input to turbine is:

Vaporizer Output Energy = Input Energy to Turbine / Vaporizer efficiency

Vaporizer Output Energy = Input Energy to Turbine / 0.5

The amount of energy to be output from solar trough heat collectors to Vaporizer is:

Solar Output Energy = Input Energy to Vaporizer / Solar trough efficiency

Solar Output Energy = Input Energy to Vaporizer / 0.75

The amount of energy can be output from solar trough by having 80% Capacity:

Solar Trough Output Capacity = Solar Output Energy / Solar trough capacity

Solar Trough Output Capacity = Solar Output Energy / 0.8

It should be mentioned the solar trough capacity to be 80% is ideal for cloud free, dust free conditions.

*Table 2: FIREBAG Location, Average daily energy needed to be input and output from each part of the process on the surface*

| Month | Daily Solar Radiation Power | Average Electricity consumption per household a month | Average Electricity consumption for 1000 household a month | Average Electricity for 1000 household per day | Input Steam Energy to Turbine for 1000 Household | Input Steam to Vaporizer for 1000 Households | Output from Solar Trough for 1000 Households | Solar Capacity 80% |
|---|---|---|---|---|---|---|---|---|
| | kWh/m2/d | kWh | kWh | kWh/day | kWh/day | kWh/day | kWh/day | kWh/day |
| January | 1.58 | 800 | 800000 | 26666.67 | 76190.49 | 152380.98 | 203174.64 | 253968.3 |
| February | 2.53 | 800 | 800000 | 26666.67 | 76190.49 | 152380.98 | 203174.64 | 253968.3 |
| March | 3.62 | 800 | 800000 | 26666.67 | 76190.49 | 152380.98 | 203174.64 | 253968.3 |
| April | 4.46 | 500 | 500000 | 16666.67 | 47619.06 | 95238.12 | 126984.16 | 158730.2 |
| May | 5.1 | 400 | 400000 | 13333.33 | 38095.23 | 76190.46 | 101587.28 | 126984.1 |
| June | 5.61 | 400 | 400000 | 13333.33 | 38095.23 | 76190.46 | 101587.28 | 126984.1 |
| July | 5.52 | 400 | 400000 | 13333.33 | 38095.23 | 76190.46 | 101587.28 | 126984.1 |
| August | 4.91 | 400 | 400000 | 13333.33 | 38095.23 | 76190.46 | 101587.28 | 126984.1 |
| September | 3.77 | 400 | 400000 | 13333.33 | 38095.23 | 76190.46 | 101587.28 | 126984.1 |
| October | 2.38 | 500 | 500000 | 16666.67 | 47619.06 | 95238.12 | 126984.16 | 158730.2 |
| November | 1.45 | 800 | 800000 | 26666.67 | 76190.49 | 152380.98 | 203174.64 | 253968.3 |
| December | 1.28 | 800 | 800000 | 26666.67 | 76190.49 | 152380.98 | 203174.64 | 253968.3 |

*(Moazami, 2020)*

In

Table 2, last column is the average heat energy needed from the solar troughs to be output in order to meet the 1000 households demand. The amount of energy is from solar radiation, therefore the last column divided by the second column, gives the area needed for solar radiation to provide this amount of energy:

Solar Energy Output = Area * Daily Solar Radiation

Area needed to have enough Solar troughs = Solar Energy Output / Daily Solar Radiation

A parabolic solar trough heat collector is a combination of 8 sections and occupy an approximate area of 50 $m^2$. The total area needed to generate enough energy to satisfy the 1000 households energy demand in December is divided by 50 $m^2$, to find the number of solar troughs needed.

From Table 3, It should be accounted for 4000 solar troughs to be installed on the surface to generate enough heat for steam production for daily electricity generation. Some of the steam amount to be utilized in daytime and the rest to be injected into depleted SAGD pads to be recovered at nighttime. It has been assumed the amount needed to be recovered from the geothermal storage (Depleted SAGD pads) is for 6 hours duration.

*Table 3: FIREBAG Location, Area and number of solar troughs needed on the surface*

| Month | Daily Solar Radiation Power | Solar Capacity 80% | m2 Solar Trough field for 1000 Households | Number of Solar Trough if each 50 m2 |
|---|---|---|---|---|
| | kWh/m2/d | kWh/day | m2/d | |
| January | 1.58 | 253968.3 | 160739.43 | 3214.79 |
| February | 2.53 | 253968.3 | 100382.73 | 2007.65 |
| March | 3.62 | 253968.3 | 70156.99 | 1403.14 |
| April | 4.46 | 158730.2 | 35589.73 | 711.79 |
| May | 5.1 | 126984.1 | 24898.84 | 497.98 |
| June | 5.61 | 126984.1 | 22635.31 | 452.71 |
| July | 5.52 | 126984.1 | 23004.37 | 460.09 |
| August | 4.91 | 126984.1 | 25862.34 | 517.25 |
| September | 3.77 | 126984.1 | 33682.78 | 673.65 |
| October | 2.38 | 158730.2 | 66693.36 | 1333.87 |
| November | 1.45 | 253968.3 | 175150.55 | 3503.01 |
| December | 1.28 | 253968.3 | 198412.73 | 3968.25 |

*(Moazami, 2020)*

To have the amount of steam to be injected and recovered whenever needed, the steam tables have been used to find the enthalpy at the temperature and pressure steam will enter and exit the steam turbine. As shown in Figure 10, it has been assumed the steam enters the steam turbine at temperature (Ti) 230 C° and pressure (Pi) 30 bar. The steam existing the turbine after mechanical energy is converted to electrical energy, is at temperature (To) 100 C° and pressure (Po) 1 bar. These assumptions make the entering steam enthalpy about 0.778 kWh/kg and the output steam from the turbine about 0.743 kWh/kg.

The mass amount of steam needed to convert enough mechanical energy into electrical energy is the total amount of steam energy needed to be input to turbine divided by the difference of the input and output steam enthalpies. The amount of energy needed for 6 hours at nighttime has been determined, then this amount divided by the enthalpies difference would give the amount of steam mass rate needed for 6 hours to be injected into geothermal heat storage and recovered when needed. The steam quality is assumed to be 85% vapor coming out of the geothermal storage.

This amount divided by 1000 kg/m3 would give the amount of steam volume (cold water equivalent) needed to be stored. Then the steam volume storage amount is computed daily. The steam volume needed to be injected and stored in December, would be the amount to account for, which would be sufficient for the other months of the year as well.

In SAGD operations, the norm is to inject 300 $m^3$/day cold water equivalent (CWE) steam into the SAGD pairs (JACOS, 2018), therefore the total amount of volume of steam to be injected and stored daily in December (column 9 in Table 4) divided by 300 $m^3$/day provides the total number of SAGD pairs to be dedicated for this microgrid. As per these assumptions and calculations (Table 4), 12 pairs needed to be allocated for the project of this size. This means a whole depleted SAGD pad to be assigned for the project of this size.

*Figure 10: FIREBAG Microgrid Steam properties across different parts of the process*

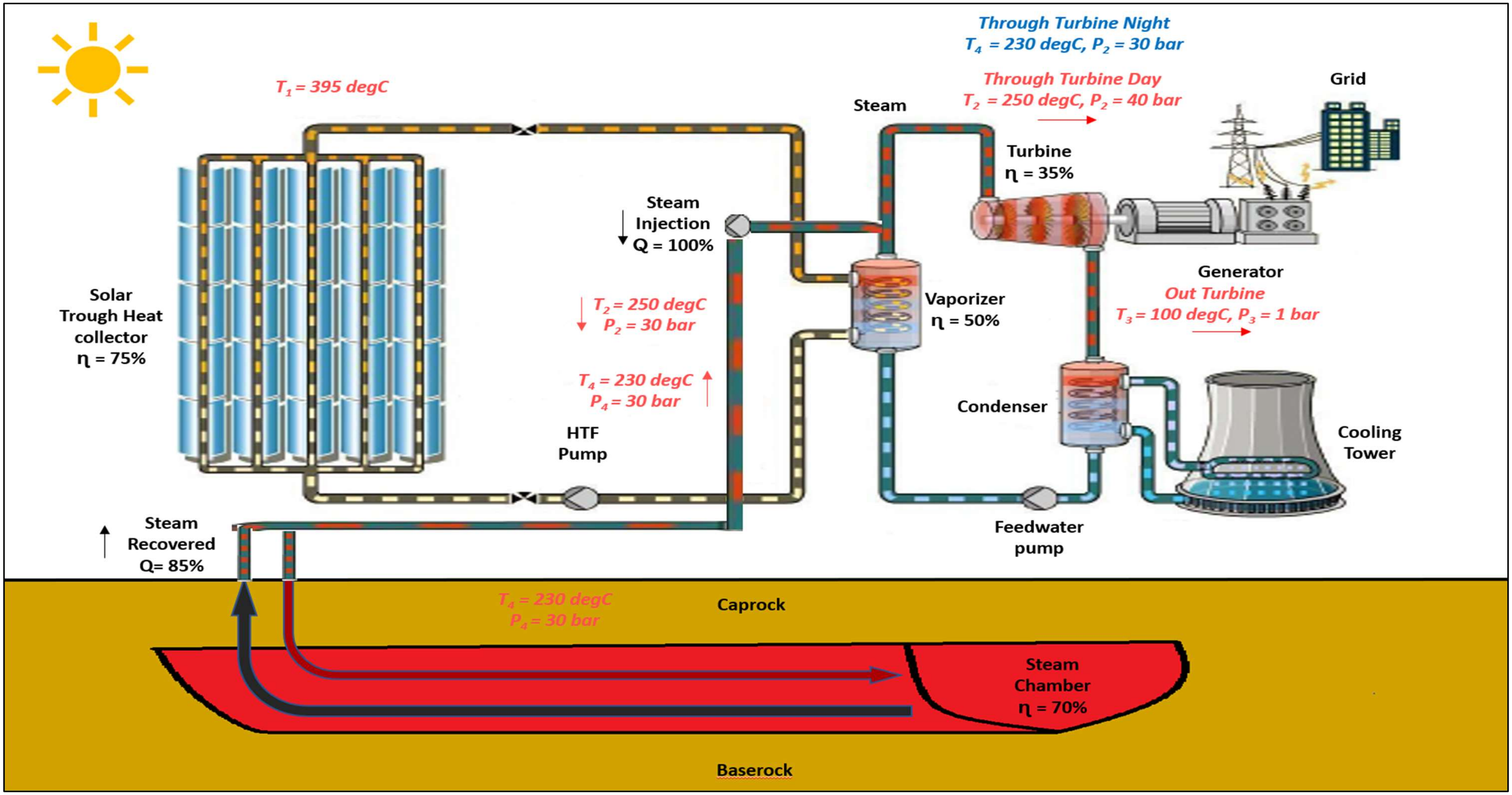


(Moazami, 2020)

*Table 4: FIREBAG Location, the amount of steam to be injected into depleted SAGD pads*

| Month | Average Electricity for 1000 household per day | Input Steam Energy to Turbine for 1000 Household | Output Steam Energy from GeoTES for 1000 Household 6hour | Output Steam Energy from GeoTES for 1000 Household 6hour, efficiency 70% | Output Steam Mass from GeoTES for 1000 Households for 6hour Ti = 230 C, Pi=30Bar Enti= 0.778 kWh/kg To = 100C, Po=1 bar Ento= 0.743 kWh/kg | Steam Mass quality of vapor 85% | Input CWE (Cold Water Equivalent) volume density = 1000 kg/m3 | Inject volume CWE (Cold Water Equivalent) per day | Inject volume CWE (Cold Water Equivalent) per day with rate 300m3/day |
|---|---|---|---|---|---|---|---|---|---|
| | kWh/day | kWh/day | kWh/ 6hour | kWh/ 6hour | kg/6hour | kg/6hr | m3/6hr | m3/day | |
| January | 26666.67 | 76190.49 | 19047.62 | 27210.89 | 777453.98 | 914651.74 | 914.65 | 3658.61 | 12.19 |
| February | 26666.67 | 76190.49 | 19047.62 | 27210.89 | 777453.98 | 914651.74 | 914.65 | 3658.61 | 12.19 |
| March | 26666.67 | 76190.49 | 19047.62 | 27210.89 | 777453.98 | 914651.74 | 914.65 | 3658.61 | 12.19 |
| April | 16666.67 | 47619.06 | 11904.76 | 17006.81 | 485908.77 | 571657.38 | 571.66 | 2286.63 | 7.62 |
| May | 13333.33 | 38095.23 | 9523.81 | 13605.44 | 388726.84 | 457325.69 | 457.33 | 1829.30 | 6.09 |
| June | 13333.33 | 38095.23 | 9523.81 | 13605.44 | 388726.84 | 457325.69 | 457.33 | 1829.30 | 6.09 |
| July | 13333.33 | 38095.23 | 9523.81 | 13605.44 | 388726.84 | 457325.69 | 457.33 | 1829.30 | 6.09 |
| August | 13333.33 | 38095.23 | 9523.81 | 13605.44 | 388726.84 | 457325.69 | 457.33 | 1829.30 | 6.09 |
| September | 13333.33 | 38095.23 | 9523.81 | 13605.44 | 388726.84 | 457325.69 | 457.33 | 1829.30 | 6.09 |
| October | 16666.67 | 47619.06 | 11904.76 | 17006.81 | 485908.77 | 571657.38 | 571.66 | 2286.63 | 7.62 |
| November | 26666.67 | 76190.49 | 19047.62 | 27210.89 | 777453.98 | 914651.74 | 914.65 | 3658.61 | 12.19 |
| December | 26666.67 | 76190.49 | 19047.62 | 27210.89 | 777453.98 | 914651.74 | 914.65 | 3658.61 | 12.19 |

*(Moazami, 2020)*

### 3.2. Geothermal District Heating

Oil and Gas is Alberta's largest industry and the main source of economy for the province. The history of the oil and gas industry in Alberta goes back to more than half a century ago. As a result, Alberta is home to immense number of active and non active wells (Reid, 2017). The drilled wells are productive for a certain amount of years of lifetime, and after that once the hydrocarbon reserves are no longer economically justifiable to continue the operation, the decommissioned wells become a hazardous risk and huge liabilities for companies and the government.

Not only the nonproducing wells are huge liabilities, these nonproducing wells are hazardous risk to both human health and the environment as they can leak. The complete abandonment of a nonproducing well is achieved, when downhole suspension is done by pulling the downhole equipment to surface, sealing the well by isolation plug or cement and surface facilities such as wellhead are completely removed to seal the well below ground level (Reid, 2017). This procedure can cost from $100,000 to $300,000 per well (Wilson, 2016).

Some of the suspended wells, specially the stripper wells which are producing high amount of water have the potential to be converted into geothermal wells for district heating applications. Converting just 10 percent of Alberta's thousands of suspended wells to geothermal heating systems can create business and work for hundreds of services and defer the high cost of abandonment for producers (Wilson, 2016). No matter how cold outside gets, the ground temperature in these formations stays around 50-60 °C.

For this capstone project, operating fields with proximity to residential areas have been investigated. Turner Valley field was selected to be a good candidate for geothermal district heating potential. Turner Valley is an old gas field in the Calgary Region, within the Municipal District of Foothills (Figure 11). The field is operating the stripper wells with more than 90% water production. The data from the decommissioned wells of this field have been used to do feasibility analysis for space heating applications for residential area within 5 km of this field location.

*Figure 11: Turner Valley Oilfield Location*

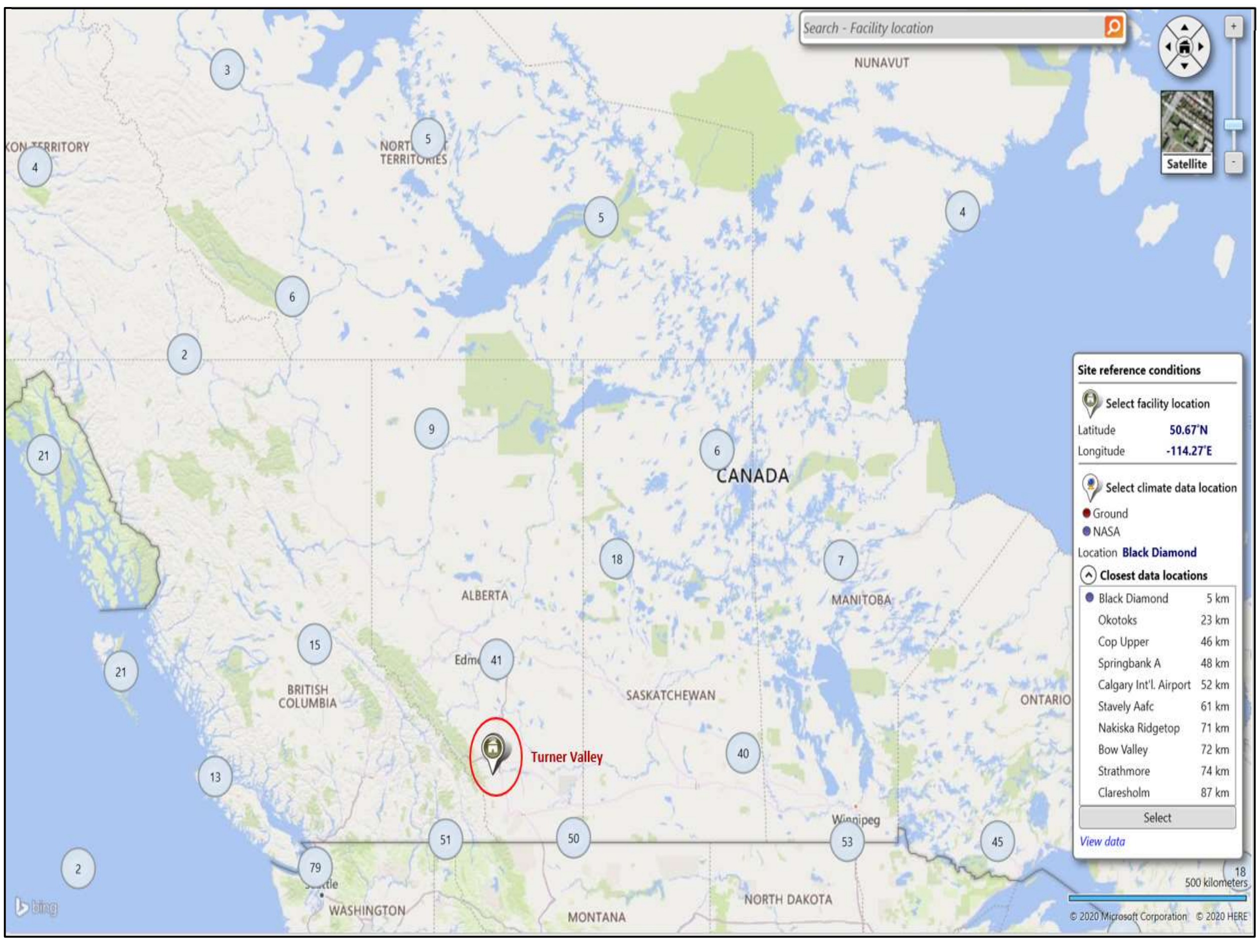


*(RetScreen, 2020)*

### 3.2.1. Geothermal heat transfer

Heat flow is the movement of heat (energy) from the interior of the Earth to the surface. As geothermal fluid rises to the surface, the heat transfer from the fluid to the surrounding rocks takes place. As discussed in previous chapters, heat transfer downhole is done through three mechanisms, radiation, conduction, and convection. When fluid moves very slowly upward, the heat energy is partially transferred to surrounding rocks conductively or to the air convectively. If fluid rises very quickly, before heat transfer is complete, hot springs or geysers can form, where normally geothermal heat is high enough for electricity generation.

Geothermal energy is not affected by weather or intermittency compared to other renewable sources. Geothermal energy can provide clean and reliable energy for several applications such as power generation, residential space heating/cooling, agricultural and industrial heating applications or for greenhouse heating. Compared to conventional geothermal operations, retrofitting the abandoned wells for geothermal operation can reduce the capital cost up to 50% (Ghoreishi-Madiseh, Templeton, Hassani, Al-Khawja, & Aflaki, 2014).

For space heating, the thermal energy from downhole formations heat exchanger can be accessed by fluid circulation through drilled wells. Then with the help of heat pumps the downhole temperature can be boosted to a desired level (Bloomquist, 2012) for space heating. The sustainability of long-term geothermal reservoirs, depends on the balance between heat extraction rate and the rate at which the geothermal heat content of the reservoir can be replaced (Ghoreishi-Madiseh, Templeton, Hassani, Al-Khawja, & Aflaki, 2014).

### 3.2.2. Heat Pumps

Heat pumps are used to transfer heat energy from a source to a destination. In Geothermal district heating geothermal heat pumps (GHP) known as GeoExchange, geothermal hot fluid acts as heat source and then heat pump interacting with the ventilation systems of the building raises the building's air temperature to a desired degree. There are 4 different types of heat pumps:

- Vertical Heat Pumps
- Horizontal Heat Pumps
- Pond Loop Heat Pumps
- Open Loop Heat Pumps

The first three mentioned above are closed loop pumps, where geothermal heat pumps circulate an antifreeze solution through the loop. The heat exchanger transfers heat between the refrigerant in the heat pump and the antifreeze solution. In open loop heat pump, the wells are used to circulate the fluid through heat pumps once the circulation is done the fluid returns to ground through the well.

In this project, open loop heat pump system has been assumed, where decommissioned oil and gas wells are converted into geothermal heating purposes. And the geothermal fluid is clean water solution with antifreeze, which meets the Alberta codes to circulate with little environmental impacts.

The heat pumps are designed to work with proper refrigerant, for this project tables for refrigerant R134a vapor compression and refrigeration system have been used. The R134a is still common but in near future would be replaced by R744. Figure 12, shows a basic schematic of refrigeration or heat pump system.

*Figure 12: Basic refrigeration or heat pump system schematic*

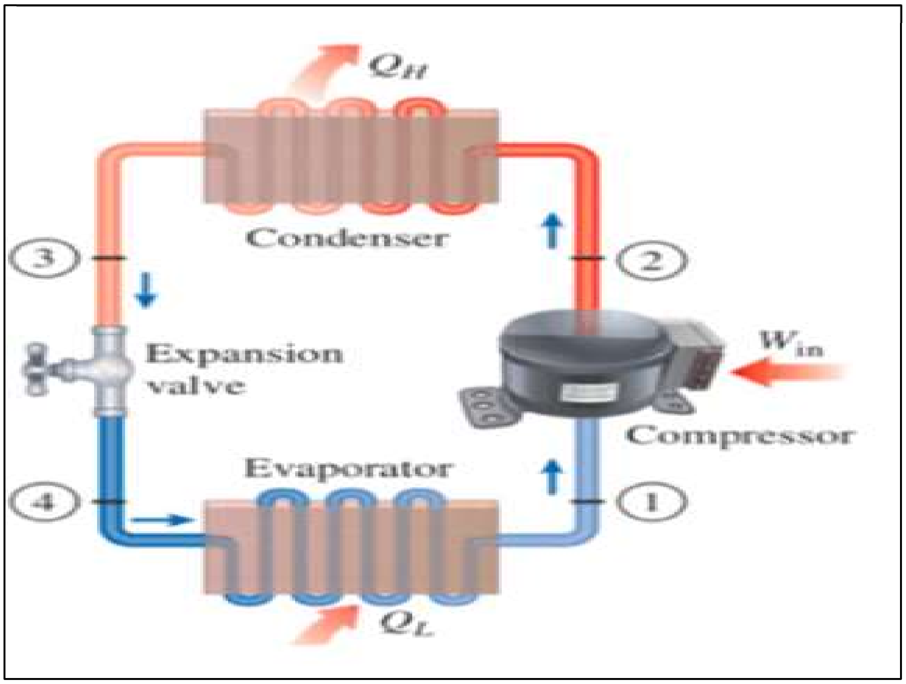


*(Xu, 2018)*

The same system can be used for heating or refrigerator. In this system, for heat pump, heat from heat source (hot geothermal fluid) being rejected in the condenser ($Q_H$), is the desired output. And if acting as refrigerator, heat being absorbed in the evaporator ($Q_L$) is the desired output. For Turner Valley location, only district heating purposes are being analyzed. As the climate during hot months of the year is cool enough and no need for cooling applications.

The basic components of geothermal heat pumps are shown in Figure 12:

- Evaporator/Vaporizer: by absorbing heat from geothermal fluid (acting as heat source), the low-pressure liquid refrigerant converts into low pressure vapor refrigerant
- Compressor: it compresses low pressure low temperature refrigerant vapor into superheated high-pressure refrigerant vapor
- Condenser: it works opposite of evaporator, it converts high pressure vapor refrigerant to high pressure refrigerant liquid
- Expansion valve: converts the high-pressure refrigerant liquid to low pressure liquid to be fed into vaporizer

The geothermal fluid travels through the geothermal well, where it absorbs the heat from the earth and then hot temperature geothermal fluid acts as heat source for the evaporator.

### 3.2.3. Drilled wells configuration in Turner Valley

The average drilled wells in Turner Valley gas field are 2000 m deep, borehole size 200mm, casing diameter 139.7 mm and tubing 88.9 mm. The wells are old and already producing with more than 90% water cut. They have a proximity to residential area, therefore a good candidate to be converted into geothermal heating purposes. The bottom hole temperature in these wells reaches around 55 °C:

$$\text{Temperature at specific depth} = \text{Temperature Gradient} * \text{Depth} + 5$$

In this project, it has been assumed the geothermal fluid enters the well from annulus, as it goes down the well it absorbs the heat, which is transferred from formation to the borehole. The fluid temperature rises and at the bottom of the well it enters the tubing. The tubing has been assumed to be a good insulator and it keeps geothermal fluid temperature around 40 °C, at the surface before it connects to the vaporizer. It has been assumed the geothermal fluid reaches vaporizer at a temperature of 40 °C and pressure of 10 bars. After heat pump process is complete the geothermal fluid going back to the well is at 26.7 °C and 7 bars (Figure 13, modified from reference).

*Figure 13: Turner Valley Location, Geothermal Heat Pump*

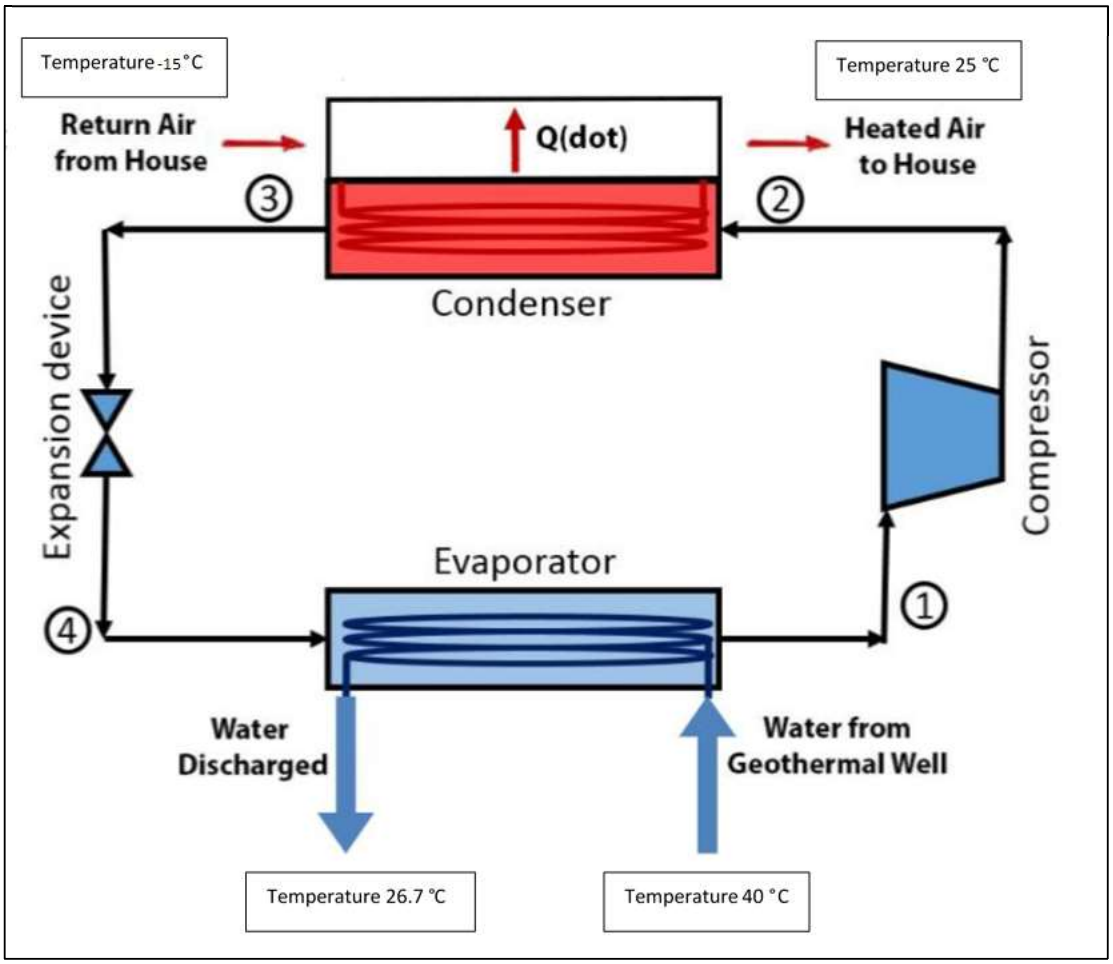


*Modified from (Urieli, 2020)*

In Turner Valley, the geothermal district heating is designed to increase the temperature of the building from average -15 °C during coldest months into 25 °C.

### 3.2.4. Designing geothermal heat pumps for an average 2000 ft2 house in Calgary

It has been assumed the average houses in Calgary are 2000 $ft^2$, with 9 ft ceiling height. Then the total volume of the house and the amount of air in that volume to be replaced by the ventilation system has been computed (Appendix B):

Average Calgary house: 2000 $ft^2$

Volume of the house: 2000 $ft^2$ * 9 ft ceiling = 18000 $ft^3$

Therefore, an average volume of 509 $m^3$, considering air density to be 1.2754 $kg/m^3$, the air mass in the house would be 650 kg. It has been assumed the ventilation, displaces 70% of the air per hour, 455 kg/hr of air to be displaced. That would be 0.1264 kg per second.

The air specific heat is 1.005 kJ/kg.K, the vent system needs to displace 0.1264 kg/s air to increase temperature from -15 to 25 °C:

$$\text{Heat Needed} = \text{Air Mass} * \text{Air Specific Heat} * \text{Temperature Difference}$$

$$\text{Heat Needed} = 0.1264 \text{ kg/s} * 1.005 \text{ kJ/kg.K} * [25-(-15)]$$

This means heat pump with capacity of 5 kW needed per household, and for 1000 household it needs to account for 5 MW heat power capacity.

To design for the heat pumps to provide this capacity, P-h diagram is plotted. The information given in Figure 13 schematic to plot four processes (1)-(2)-(3)-(4)-(1) on the P-h diagram (Figure 14).

*Figure 14: Turner Valley Location, Heat Pump P-h Diagram*

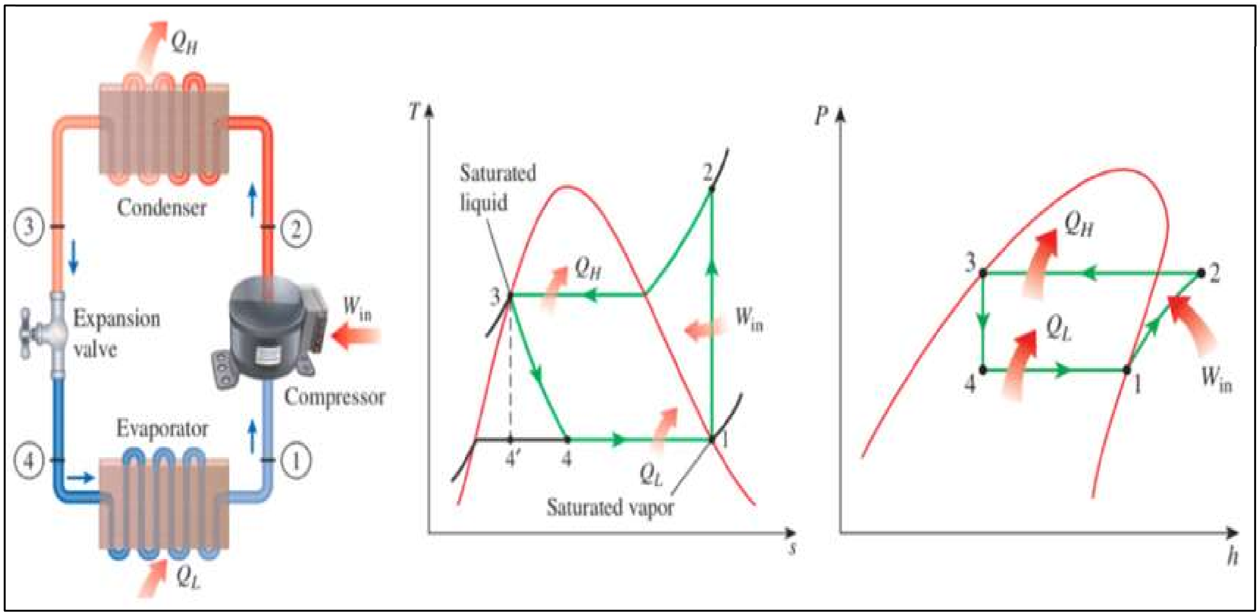


*(Xu, 2018)*

The fluid enters and exists the condenser from state (2) to state (3) at high pressure of 10 bars. The fluid enters the vaporizer at state (4) at low temperature of 26.7 °C and exists the vaporizer at state (1) as a saturated vapor at temperature 40 °C. The state (3) and (4) have equal enthalpy (h3 = h4). The R134a refrigerant tables are used to do all calculations for the heat pump design (Table 5).

- State (1): Low pressure vapor refrigerant Enthalpy @ 1.6 bars, h1 = 241.1 kJ/kg
- State (2): Superheated high-pressure vapor refrigerant Enthalpy @10 bars, h2 = 271 kJ/kg
- State (3): Enthalpy is equal to state (4) h3 = h4
- State (4): Low pressure temperature refrigerant liquid Enthalpy @ 26.7 °C, h4 = 88.8 kJ/kg

*Table 5: R134a, Refrigerant parameters used for P-h diagram*

| Pressure | Temp | volume (m^3/kg) | | enthalpy (kJ/kg) | | | entropy (kJ/kg.K) | | |
|---|---|---|---|---|---|---|---|---|---|
| kPa | °C | vf | vg | hf | hfg | hg | sf | sfg | sg |
| 60 | -36.9 | 0.00071 | 0.3112 | 3.9 | 223.9 | 227.8 | 0.0164 | 0.9481 | 0.9645 |
| 80 | -31.1 | 0.000719 | 0.2376 | 11.3 | 220.2 | 231.5 | 0.0472 | 091 | 0.9572 |
| 100 | -26.4 | 0.000726 | 0.1926 | 17.3 | 217.2 | 234.5 | 0.072 | 0.8799 | 0.9519 |
| 120 | -22.3 | 0.000732 | 0.1621 | 22.5 | 214.5 | 237 | 0.0928 | 0.855 | 0.9478 |
| 140 | -18.8 | 0.000738 | 0.1402 | 27.1 | 212.1 | 239.2 | 0.111 | 0.8337 | 0.9446 |
| 160 | -15.6 | 0.000744 | 0.1235 | 31.2 | 209.9 | 241.1 | 0.127 | 0.815 | 0.942 |
| 180 | -12.7 | 0.000749 | 0.1104 | 35 | 207.9 | 242.9 | 0.1415 | 0.7982 | 0.9397 |
| 200 | -10.1 | 0.000753 | 0.0999 | 38.5 | 206 | 244.5 | 0.1547 | 0.7831 | 0.9378 |
| 220 | -7.6 | 0.000758 | 0.0912 | 41.7 | 204.3 | 245.9 | 0.1668 | 0.7693 | 0.9361 |
| 240 | -5.4 | 0.000762 | 0.0839 | 44.7 | 202.6 | 247.3 | 0.178 | 0.7566 | 0.9347 |
| 260 | -3.2 | 0.000766 | 0.0777 | 47.5 | 201 | 248.6 | 0.1885 | 0.7448 | 0.9333 |
| 280 | -1.2 | 0.00077 | 0.0724 | 50.2 | 199.5 | 249.7 | 0.1984 | 0.7338 | 0.9322 |
| 300 | 0.7 | 0.000774 | 0.0677 | 52.8 | 198.1 | 250.9 | 0.2077 | 0.7234 | 0.9311 |
| 320 | 2.5 | 0.000777 | 0.0636 | 55.2 | 196.7 | 251.9 | 0.2165 | 0.7137 | 0.9301 |
| 340 | 4.2 | 0.000781 | 0.06 | 57.5 | 195.4 | 252.9 | 0.2248 | 0.7044 | 0.9293 |
| 360 | 5.8 | 0.000784 | 0.0567 | 59.8 | 194.1 | 253.8 | 0.2328 | 0.6956 | 0.9284 |
| 400 | 8.9 | 0.000791 | 0.0512 | 64 | 191.6 | 255.6 | 0.2477 | 0.6793 | 0.927 |
| 500 | 15.7 | 0.000806 | 0.0411 | 73.4 | 186 | 259.3 | 0.2803 | 0.6438 | 0.9241 |
| 600 | 21.6 | 0.00082 | 0.0343 | 81.5 | 180.9 | 262.4 | 0.3081 | 0.6138 | 0.9219 |
| 700 | 26.7 | 0.000833 | 0.0294 | 88.8 | 176.2 | 265.1 | 0.3324 | 0.5876 | 0.92 |
| 800 | 31.3 | 0.000846 | 0.0256 | 95.5 | 171.8 | 267.3 | 0.3541 | 0.5643 | 0.9184 |
| 900 | 35.5 | 0.000858 | 0.0227 | 101.6 | 167.7 | 269.3 | 0.3739 | 0.5431 | 0.917 |
| 1000 | 39.4 | 0.00087 | 0.0203 | 107.4 | 163.7 | 271 | 0.392 | 0.5237 | 0.9157 |
| 1200 | 46.3 | 0.000894 | 0.0167 | 117.8 | 156.1 | 273.9 | 0.4245 | 0.4886 | 0.9131 |
| 1400 | 52.4 | 0.000917 | 0.0141 | 127.3 | 148.9 | 276.2 | 0.4533 | 0.4573 | 0.9106 |
| 1600 | 57.9 | 0.00094 | 0.0121 | 136 | 141.9 | 277.9 | 0.4792 | 0.4287 | 0.908 |
| 1800 | 62.9 | 0.000964 | 0.0106 | 144.1 | 135.1 | 279.2 | 0.5031 | 0.402 | 0.9051 |
| 2000 | 67.5 | 0.000989 | 0.0093 | 151.8 | 128.3 | 280.1 | 0.5252 | 0.3767 | 0.902 |
| 2500 | 77.6 | 0.001057 | 0.0069 | 169.7 | 111.2 | 280.9 | 0.5755 | 0.317 | 0.8925 |
| 3000 | 86.2 | 0.001141 | 0.0053 | 186.6 | 92.6 | 279.2 | 0.6215 | 0.2578 | 0.8792 |

*(R134a - Pressure Table, 2008)*

From P-h diagram plot, the system coefficient of performance is considered, by comparing the enthalpy differences of the compressor (State (1)-(2)), to of the condenser (State (2)-(3)). Each component has been separated and the energy equation has been applied. The work done in the condenser is the difference between enthalpy (3), (2) multiplied by mass rate:

$$Q_H = \text{Mass flow rate of refrigerant} * (h_2 - h_3)$$

$$\text{Mass flow rate of refrigerant} = \frac{4}{(271 - 88.8)}$$

$$\text{Mass flow rate of refrigerant} = 0.02788 \text{ kg/s}$$

Work done by the compressor ($W_{in}$) to transfer this amount of mass flow rate of refrigerant, is the mass flow rate multiplied by h2, h1 differences in enthalpy:

$$W_{in} = \text{Mass flow rate of refrigerant} * (h_2 - h_1)$$

$$W_{in} = 0.02788 * (271 – 241.1)$$

$$W_{in} = 0.8338 \text{ kW}$$

The heat absorbed from the geothermal fluid in the vaporizer, is the difference in enthalpy h1 and h4 multiplied by the mass rate:

$$Q_H = \text{Mass flow rate of refrigerant} * (h_1 - h_4)$$

$$Q_H = 0.02788 * (241.1 - 88.8)$$

$$Q_H = 4.247 \text{ kW}$$

The amount of mass rate of geothermal fluid to provide the amount of work $Q_H$, is computed by knowing the specific heat of geothermal fluid (water) at temperature it enters and exits the vaporizer:

Specific Heat water = 4.186 J/g.C

$SP_{in}$ = 4.186 * 40 °C = 167.4 J/g or kJ/kg

$SP_{out}$ = 4.186 * 26.7 °C = 111.76 J/g or kJ/kg

$$\text{Mass rate of geothermal fluid} = \frac{QH}{(SPout - SPin)}$$

$$= \frac{4.247}{(167.4 - 111.76)}$$

$$= 0.07633 \text{ kg/s}$$

This mass flow rate is needed for each heat pump, for 1000 households, it has been assumed 50 heat pumps for cluster of 20 houses. To interact with heat exchange stations and the buildings' ventilation system.

### 3.2.5. Heat Transfer Model

Geothermal fluid enters the drilled well from anulus at temperature of 26.7 °C (shown as blue in Figure 1Figure 15). As the fluid travels down the annulus, initially it loses its heat at the top to the surrounding formations where the average surface temperature is assumed to be 5 °C. As the formation temperature increases with depth, the geothermal fluid starts to warm up, and enters the tubing from bottom of the well (shown as red in Figure 15).

*Figure 15: Heat Transfer*

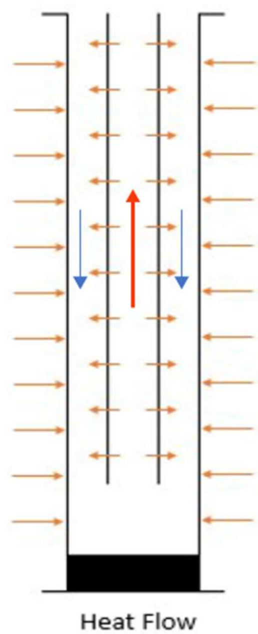


*(Reid, 2017)*

To model for the heat transfer of the formations into geothermal fluid, and the maximum attainable temperature, the Holman heat transfer book (Holman, 2009) and the capstone report by Jennifer Reid for SEDV (Reid, 2017) was used as reference. (Appendix C).

Specific Heat transfer:

$$c = 3\,e^{-5}\,(Temp)^2 - 0.0023\,(Temp) + 4.2186$$

Geothermal fluid density:

$$\rho = -0.0041(Temp)^2 - 0.0324\,(Temp) + 999.93$$

Geothermal fluid viscosity:

$$\mu = 3.31\,e^{-7}(Temp)^2 - 4.07\,e^{-5}\,(Temp) + 1.72\,e^{-3}$$

Thermal conductivity or k value:

$$k = -9.93\,e^{-7}(Temp)^2 + 2.08\,e^{-3}\,(Temp) + 5.66\,e^{-1}$$

Peclet number, Pr value:

$$Pr = 0.0027\,(Temp)^2 - 0.3257\,(Temp) + 12.717$$

Reynold’s number and hydraulic diameter:

$$Re = \frac{4m'}{\pi\,(D_o + D_i)\mu}$$

Turbulent flow, Nu is solved for using the Dittus-Boelter relation:

$$Nu = 0.023\,Re^{0.8}\;Pr^{0.4}$$

The $h_o$ is solved for using:

$$h_o = \frac{Nu\,k}{D_h}$$

Heat transfer from formation is calculated by:

$$Q' = 2\pi\, r_o\, h_o\, (T_\infty - T_i)\, \Delta z$$

Temperature in the annulus:

$$T_\infty = \frac{Q'}{(m'c\, \Delta z)} + T_i$$

Based on these assumptions and the calculations, the formation and geothermal fluid temperatures profiles are shown in Figure 16. The formation temperature shown in blue increases with depth, and the geothermal fluid temperature in red initially loses heat to surrounding formations, as it has higher temperature compared to the surrounding formations, and once formation temperature increases with depth the heat starts to transfer from formations to the geothermal fluid and increase its temperature.

*Figure 16: Formation and Geothermal fluid Temperature profile*

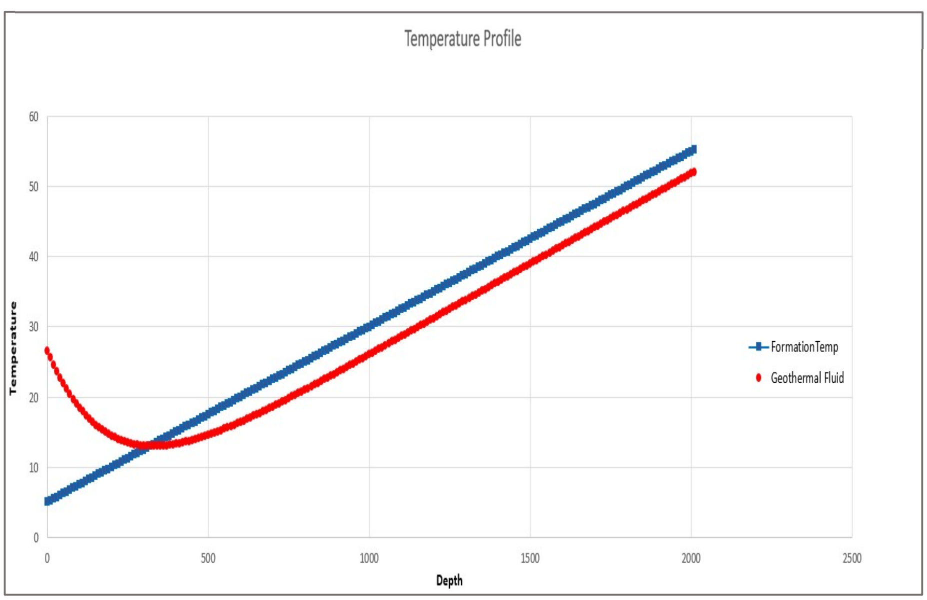


*(Moazami, 2020)*

It has been assumed the geothermal fluid entering the drilled well from anulus and after warming up traveling down to enter the tubing from the bottom of the hole. The tubing heat loss was assumed to be negligible and at the surface the hot geothermal fluid existing the tubing to stay around 40 °C to interact with the heat pump acting as the heat source. It was assumed the geothermal fluid to exit the tubing at 10 kg/s mass flow rate (m'), and 20 depleted wells with configuration listed in Table 6 to be employed for 1000 households heat energy demand in Turner Valley with power capacity of 5 MW.

*Table 6: Turner Valley, Depleted Wellbore configuration*

| Wellbore Depth | Bit Size | Casing Size | Tubing Size | Bottom Hole Temp |
|---|---|---|---|---|
| m | mm | mm | mm | °C |
| 2000 | 200 | 139.7 | 88.9 | 55 |

*(Moazami, 2020)*

The number of the wells are assumed to be 20 with mass flow rate of 10 kg/s, to provide enough hot geothermal fluid for 50 heat pumps, each heat pump is used for 20 building cluster and heat exchange station. The residential area in Turner Valley is assumed to be within 5 km of this geothermal heating facility. And the building distance to the heat pumps and heat exchange stations to be 500 m. A 10% growth margin has been accounted for in the number of houses in the neighborhood. This number of wells and flow rate is assumed to be sufficient to account for the heat loss throughout the process and in the geothermal pipes.

## Chapter 4: Economics and cost benefit analysis

The two models of, FIREBAG 100% renewable microgrid with geothermal heat storage and the Turner Valley geothermal district heating were assumed to last 20 years lifetime and modelled in RetScreen (RetScreen, 2020), to do analysis on the economics and cost benefit analysis of the two projects.

### 4.1. FIREBAG 100% renewable microgrid with geothermal heat storage

As explained in the previous section, for a 1 MW capacity microgrid to generate 7GWh electricity annually, solar trough heat collectors are used as heat source, therefore, 4000 solar troughs needed to be installed in the FIREBAG location and a complete SAGD depleted pad to be dedicated for heat storage for night time recovery.

The main investment to account for is the solar troughs installation and the Rankine cycle. Based on RetScreen financial analysis, an initial investment of $6.5 million is needed for 4000 solar troughs installation. After deducting the annual costs from the revenue generated from electricity generation and carbon tax credit, an annual positive cash flow of $ 177k would remain for the project owner. The LOCE would be around 12 cents/kWh.

*Figure 17: RetScreen Financial Analysis, for renewable 1 MW microgrid with geothermal storage*

**RETScreen - Financial Analysis**

**Financial parameters**

| | | |
|---|---|---|
| **General** | | |
| Fuel cost escalation rate | | 2% |
| Inflation rate | % | 2% |
| Discount rate | % | 9% |
| Reinvestment rate | % | 9% |
| Project life | yr | 20 |
| **Finance** | | |
| Incentives and grants | $ | |
| Debt ratio | % | 70% |
| Debt | $ | 4,550,000 |
| Equity | $ | 1,950,000 |
| Debt interest rate | % | 7% |
| Debt term | yr | 15 |
| Debt payments | $/yr | 499,566 |
| **Income tax analysis** | | ☐ |

**Annual revenue**

| | | |
|---|---|---|
| **Electricity export revenue** | | |
| Electricity exported to grid | MWh ▾ | 7,008 |
| Electricity export rate | $/kWh ▾ | 0.10 |
| Electricity export revenue | $ | 700,800 |
| Electricity export escalation rate | % | 2% |
| **GHG reduction revenue** | | |
| Net GHG reduction | $tCO_2$/yr | 3,721 |
| Net GHG reduction - 20 yrs | $tCO_2$ | 74,425 |
| GHG reduction credit rate | $/$tCO_2$ | 30 |
| GHG reduction revenue | $ | 111,637 |
| GHG reduction credit duration | yr | 20 |
| Net GHG reduction - 20 yrs | $tCO_2$ | 74,425 |
| GHG reduction credit escalation rate | % | 2% |
| **Other revenue (cost)** | | ☐ |
| **Clean Energy (CE) production revenue** | | ☐ |

**Costs | Savings | Revenue**

| | | | |
|---|---|---|---|
| **Initial costs** | | | |
| Initial cost | 100% | $ | 6,500,000 |
| **Total initial costs** | **100%** | $ | **6,500,000** |
| **Yearly cash flows - Year 1** | | | |
| **Annual costs and debt payments** | | | |
| O&M costs (savings) | | $ | 135,000 |
| Debt payments - 15 yrs | | $ | 499,566 |
| **Total annual costs** | | **$** | **634,566** |
| **Annual savings and revenue** | | | |
| Electricity export revenue | | $ | 700,800 |
| GHG reduction revenue - 20 yrs | | $ | 111,637 |
| Other revenue (cost) | | $ | 0 |
| CE production revenue | | $ | 0 |
| **Total annual savings and revenue** | | **$** | **812,437** |
| **Net yearly cash flow - Year 1** | | **$** | **177,872** |

**Financial viability**

| | | |
|---|---|---|
| Pre-tax IRR - equity | % | 14.7% |
| Pre-tax MIRR - equity | % | 11.8% |
| Pre-tax IRR - assets | % | 2.7% |
| Pre-tax MIRR - assets | % | 5.3% |
| Simple payback | yr | 9.6 |
| Equity payback | yr | 8.1 |
| Net Present Value (NPV) | $ | 1,277,142 |
| Annual life cycle savings | $/yr | 139,906 |
| Benefit-Cost (B-C) ratio | | 1.7 |
| Debt service coverage | | 1.4 |
| GHG reduction cost | $/$tCO_2$ | -37.60 |
| Energy production cost | $/kWh ▾ | 0.116 |

**Yearly cash flows**

| Year | Pre-tax | Cumulative |
|---|---|---|
| # | $ | $ |
| 0 | -1,950,000 | -1,950,000 |
| 1 | 191,421 | -1,758,579 |
| 2 | 205,240 | -1,553,339 |
| 3 | 219,336 | -1,334,002 |
| 4 | 233,715 | -1,100,288 |
| 5 | 248,380 | -851,908 |
| 6 | 263,339 | -588,569 |
| 7 | 278,597 | -309,972 |
| 8 | 294,160 | -15,811 |
| 9 | 310,035 | 294,224 |
| 10 | 326,227 | 620,451 |
| 11 | 342,743 | 963,193 |
| 12 | 359,589 | 1,322,782 |
| 13 | 376,772 | 1,699,554 |
| 14 | 394,299 | 2,093,853 |
| 15 | 412,176 | 2,506,029 |
| 16 | 929,976 | 3,436,006 |
| 17 | 948,576 | 4,384,582 |
| 18 | 967,547 | 5,352,129 |
| 19 | 986,898 | 6,339,027 |
| 20 | 1,006,636 | 7,345,664 |

*(RetScreen, 2020)*

The Cash flow analysis for FIREBAG 100% renewable microgrid (Figure 18), indicates positive cumulative cash flow and revenue generation.

*Figure 18: RetScreen Cash flow analysis for FIREBAG location*

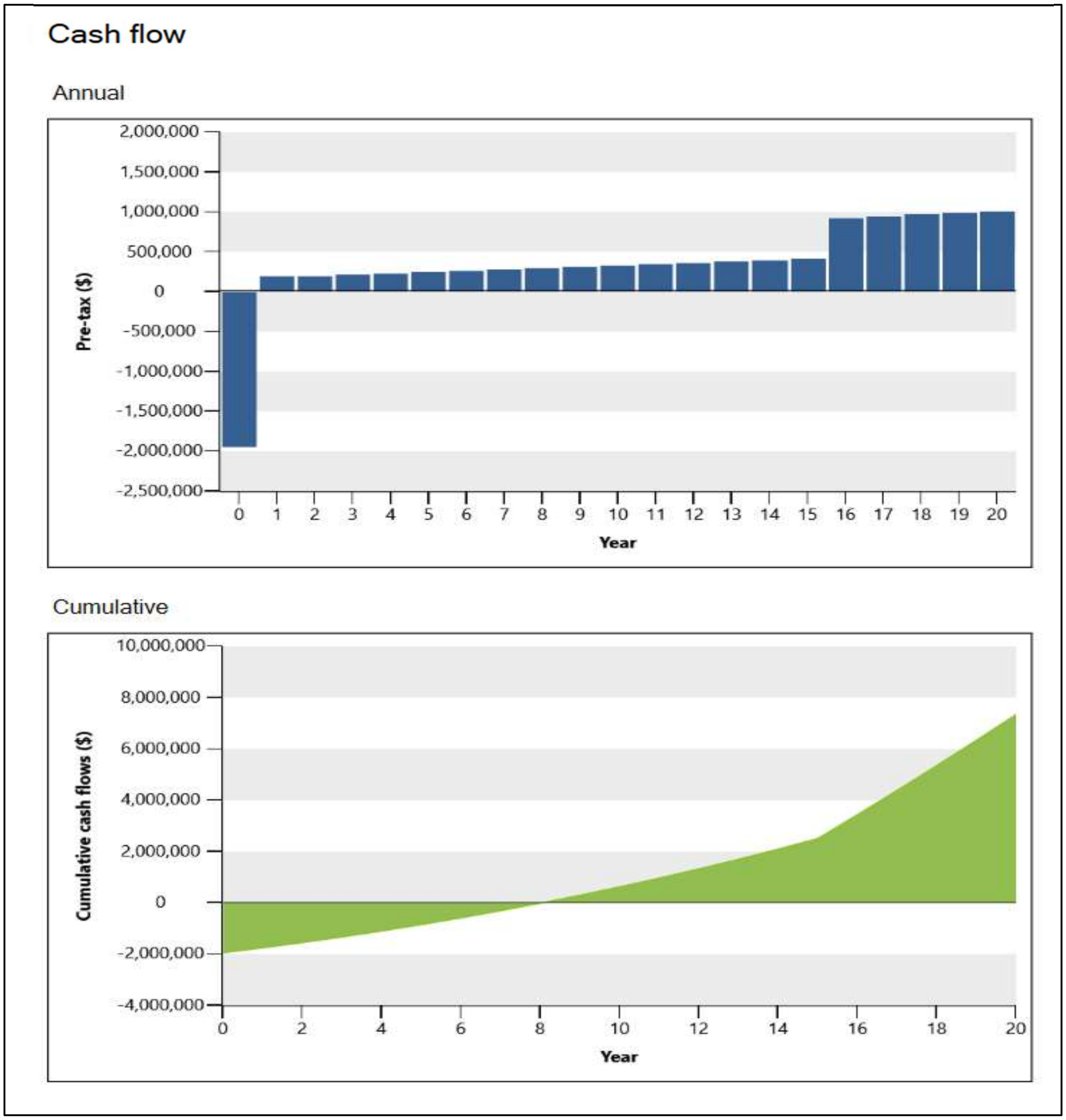


*(RetScreen, 2020)*

### 4.2. Turner Valley geothermal district heating

For Turner Valley, a geothermal facility with 5MW power capacity is needed to provide nearby 1000 households heating energy of 18.9 GWh annually. The main investments needed for this facility of this size are mainly for geothermal underground piping, heat pumps and heat exchange stations. The size of the facility and distribution of the individual buildings designed in this study, need an initial investment of $30 million. It was assumed the project owner to receive rebate from replacing natural gas furnaces and retrofitting 20 decommissioned wells into geothermal. That makes the initial investment into than $21 million.

Based on RetScreen financial analysis, after deducting the revenue generated from the annual total cost, the Turner Valley Geothermal district heating facility still would cost $1.2 million annually for the project owner, which would not be economical. The cash flow analysis shows negative cash flow through 20 years time of the project.

*Figure 19: RetScreen Financial Analysis, for geothermal district heating of 5MW capacity*

**RETScreen - Financial Analysis**

**Financial parameters**

| General | | |
|---|---|---|
| Fuel cost escalation rate | % | 2% |
| Inflation rate | % | 2% |
| Discount rate | % | 9% |
| Reinvestment rate | % | 9% |
| Project life | yr | 20 |

| Finance | | |
|---|---|---|
| Incentives and grants | $ | |
| Debt ratio | % | 70% |
| Debt | $ | 14,691,757 |
| Equity | $ | 6,296,467 |
| Debt interest rate | % | 7% |
| Debt term | yr | 15 |
| Debt payments | $/yr | 1,613,076 |

**Income tax analysis** ☐

**Annual revenue**

| GHG reduction revenue | | |
|---|---|---|
| Net GHG reduction | $tCO_2/yr$ | 2,597 |
| Net GHG reduction - 20 yrs | $tCO_2$ | 51,936 |
| GHG reduction credit rate | $\$/tCO_2$ | 30 |
| GHG reduction revenue | $ | 77,904 |
| GHG reduction credit duration | yr | 20 |
| Net GHG reduction - 20 yrs | $tCO_2$ | 51,936 |
| GHG reduction credit escalation rate | % | 2% |

**Customer premium income (rebate)** ☐

**Other revenue (cost)** ☐

**Costs | Savings | Revenue**

| Initial costs | | | |
|---|---|---|---|
| Initial cost | 143% | $ | 29,988,224 |
| Nat Gas Furnaces | -23.8% | $ | -5,000,000 |
| Well decomissiong | -19.1% | $ | -4,000,000 |
| **Total initial costs** | **100%** | $ | **20,988,224** |

**Yearly cash flows - Year 1**

| Annual costs and debt payments | | |
|---|---|---|
| O&M costs (savings) | $ | 720,900 |
| Fuel cost - proposed case | $ | 314,975 |
| Debt payments - 15 yrs | $ | 1,613,076 |
| **Total annual costs** | **$** | **2,648,951** |

| Annual savings and revenue | | |
|---|---|---|
| Fuel cost - base case | $ | 1,111,676 |
| GHG reduction revenue - 20 yrs | $ | 77,904 |
| Customer premium income (rebate) | $ | 0 |
| Other revenue (cost) | $ | 0 |
| **Total annual savings and revenue** | **$** | **1,189,580** |
| **Net yearly cash flow - Year 1** | **$** | **-1,459,371** |

**Financial viability**

| | | |
|---|---|---|
| Pre-tax IRR - equity | % | Negative |
| Pre-tax MIRR - equity | % | -12.3% |
| Pre-tax IRR - assets | % | Negative |
| Pre-tax MIRR - assets | % | -14.8% |
| Simple payback | yr | 137 |
| Equity payback | yr | > project |
| Net Present Value (NPV) | $ | -17,653,097 |
| Annual life cycle savings | $/yr | -1,933,835 |
| Benefit-Cost (B-C) ratio | | -1.8 |
| Debt service coverage | | 0.1 |
| GHG reduction cost | $\$/tCO_2$ | 745 |

**Yearly cash flows**

| Year | Pre-tax | Cumulative |
|---|---|---|
| # | $ | $ |
| 0 | -6,296,467 | -6,296,467 |
| 1 | -1,456,297 | -7,752,764 |
| 2 | -1,453,161 | -9,205,925 |
| 3 | -1,449,963 | -10,655,887 |
| 4 | -1,446,700 | -12,102,588 |
| 5 | -1,443,373 | -13,545,961 |
| 6 | -1,439,979 | -14,985,939 |
| 7 | -1,436,517 | -16,422,456 |
| 8 | -1,432,986 | -17,855,442 |
| 9 | -1,429,384 | -19,284,826 |
| 10 | -1,425,710 | -20,710,536 |
| 11 | -1,421,963 | -22,132,499 |
| 12 | -1,418,140 | -23,550,639 |
| 13 | -1,414,242 | -24,964,881 |
| 14 | -1,410,265 | -26,375,146 |
| 15 | -1,406,209 | -27,781,355 |
| 16 | 211,004 | -27,570,350 |
| 17 | 215,225 | -27,355,126 |
| 18 | 219,529 | -27,135,597 |
| 19 | 223,920 | -26,911,677 |
| 20 | 228,398 | -26,683,279 |

*(RetScreen, 2020)*

*Figure 20: RetScreen Cash flow analysis for FIREBAG location*

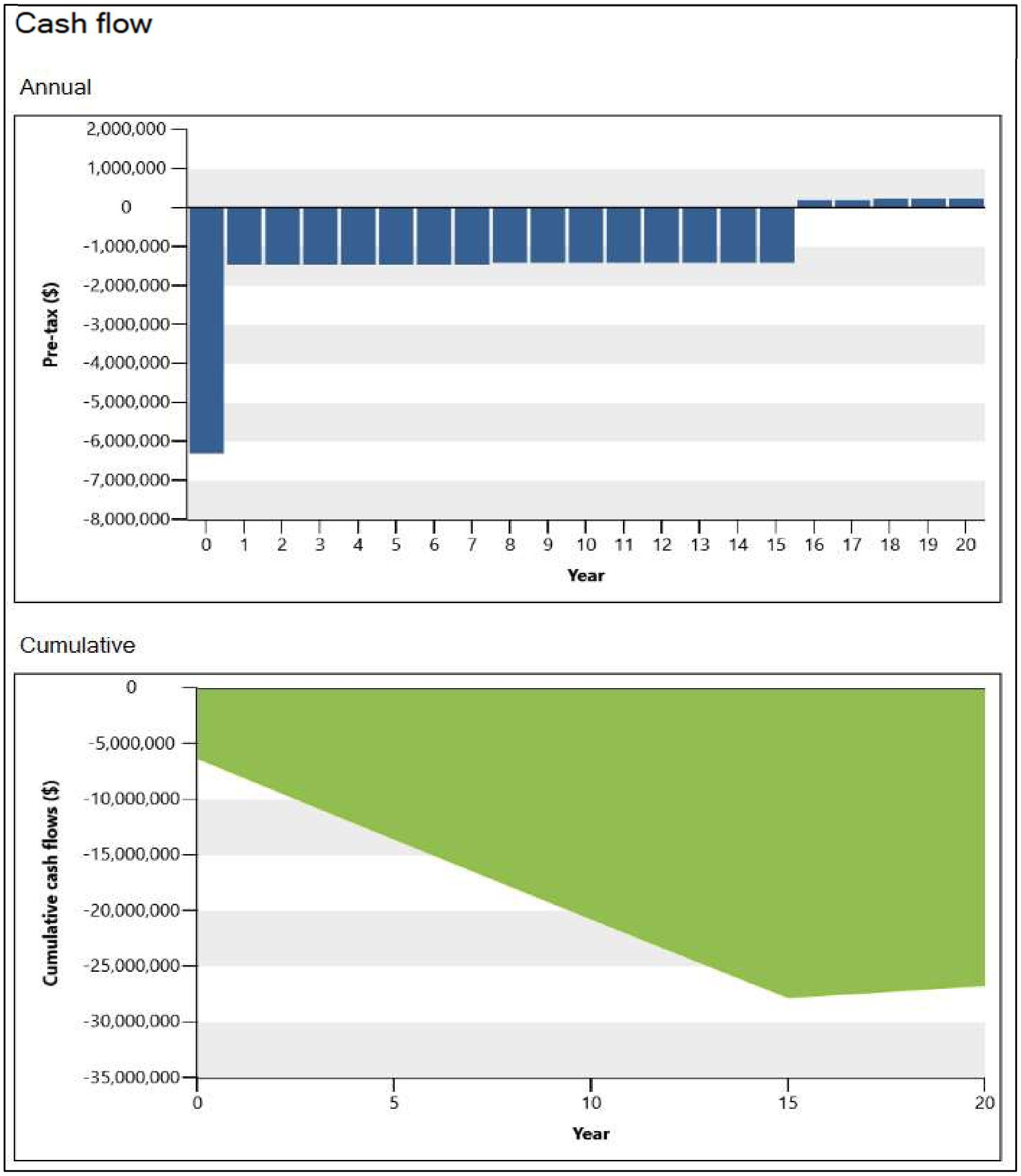


*(RetScreen, 2020)*

## Chapter 5: GHG Emission Reductions

These two proposed projects would replace the fossil fuels. The 100% renewable microgrid with geothermal storage would replace electricity from fossil fuels with solar heat and geothermal heat electricity generation. The geothermal district heating would replace heat energy from fossil fuels with the Earth's thermal energy. The RetScreen simulation shows tremendous amount of $CO_2$ reduction by implementing these projects.

### 5.1. FIREBAG 100% renewable microgrid with geothermal heat storage

The FIREBAG 100% renewable microgrid facility, would reduce more than 4,000 $tCO_2$ annually in GHG emissions, which is 93% less than the base case if natural gas is used. The 7% emission is assumed to be for electricity transmission to grid. This amount of $CO_2$ reduction is equivalent to 757 cars being removed from the vehicle fleet. This can generate more than $111k revenue annually in carbon tax credit, if GHG reduction credit rate would be 30 $/tCO_2$.

### 5.2. Turner Valley geothermal district heating

The Turner Valley geothermal district heating facility would reduce more than 2,800 $tCO_2$ annually in GHG emissions, which is 72% less than the base case if natural gas is used. The majority of the GHG emission for this project would be for the energy needed to operate the heat pumps. This amount of $CO_2$ reduction is equivalent to 528 cars being removed from the vehicle fleet. This can generate more than $77k revenue annually in carbon tax credit.

*Figure 21: FIREBAG 100% renewable microgrid with geothermal heat storage*

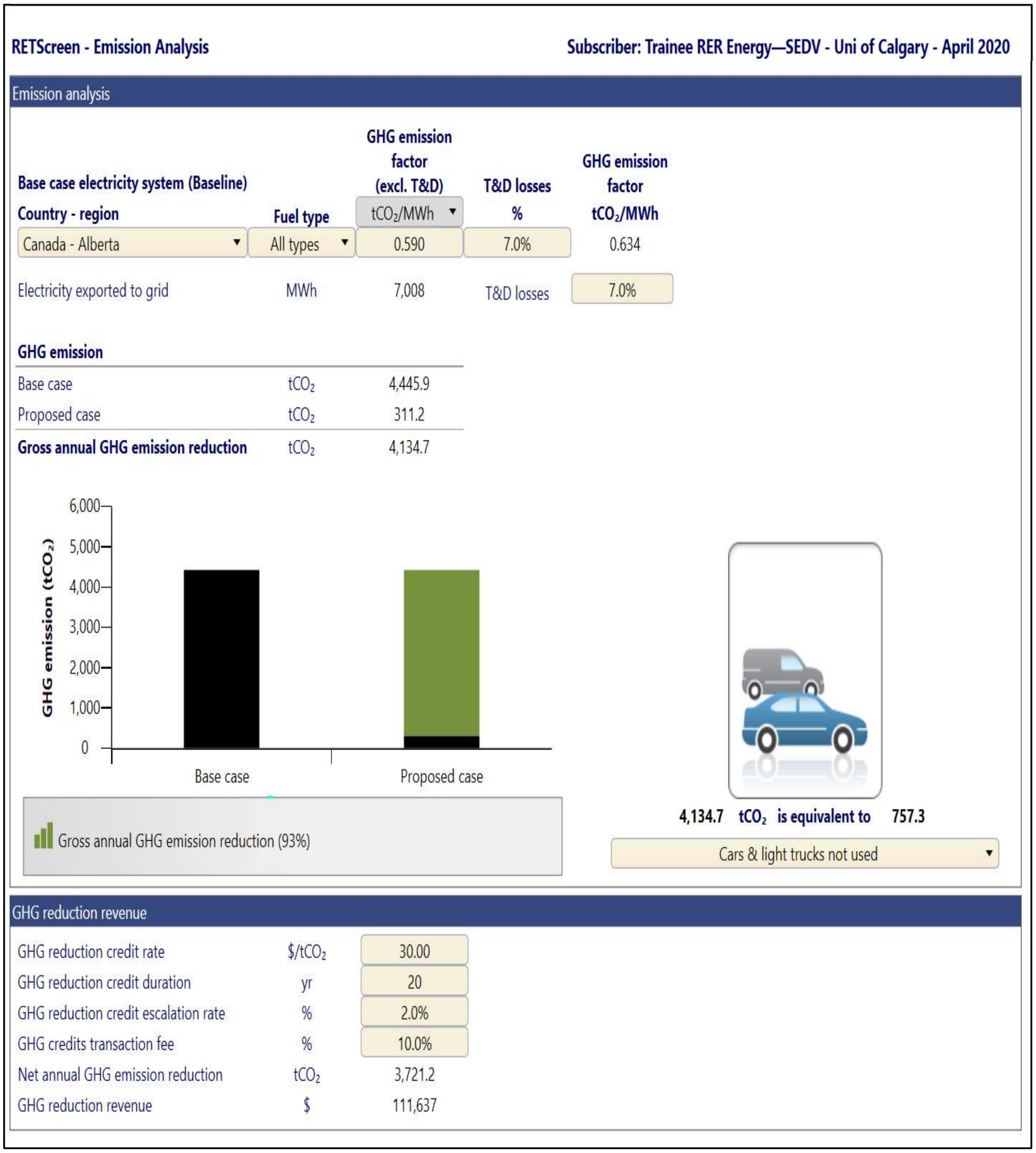


*(RetScreen, 2020)*

*Figure 22: Turner Valley geothermal district heating*

**RETScreen - Emission Analysis** | **Subscriber: Trainee RER Energy—SEDV - Uni of Calgary - April 2020**

Emission analysis

**GHG emission**

| | | |
|---|---|---|
| Base case | $tCO_2$ | 4,026.0 |
| Proposed case | $tCO_2$ | 1,140.7 |
| **Gross annual GHG emission reduction** | $tCO_2$ | 2,885.3 |

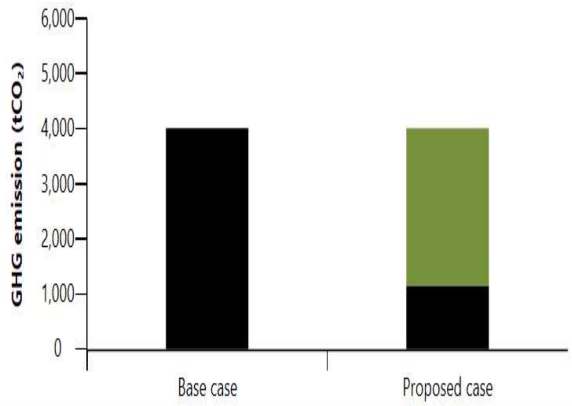


Gross annual GHG emission reduction (72%)

**2,885.3 $tCO_2$ is equivalent to 528.4**

Cars & light trucks not used

GHG reduction revenue

| | | |
|---|---|---|
| GHG reduction credit rate | $/tCO_2$ | 30.00 |
| GHG reduction credit duration | yr | 20 |
| GHG reduction credit escalation rate | % | 2.0% |
| GHG credits transaction fee | % | 10.0% |
| Net annual GHG emission reduction | $tCO_2$ | 2,596.8 |
| GHG reduction revenue | $ | 77,904 |

*(RetScreen, 2020)*

# Chapter 6: Conclusions

Based on this research both proposed cases in FIREBAG and Turner Valley, for geothermal heat storage and district heating recovery are feasible. The size of the facilities and infrastructure from oil and gas to be converted into geothermal are technically reasonable and practical. The GHG reduction is guaranteed from implementation of both projects. The FIREBAG 100% renewable microgrid with geothermal storage for 1000 households' electricity demand is economical and this project would generate positive cash flow for the project owner. On the other hand, the Turner Valley geothermal district heating facility for 1000 households' heat energy demand is not economical. However, it should be mentioned if the size of the project is modified to smaller scale where a lower number of heat pumps and geothermal piping amount is needed, this project can become economical. The geothermal district heating is also ideal for space heating purposes such as a nearby agricultural greenhouse or a factory, where heat can be provided for a huge space rather than massive investment needed for individual buildings or houses.

## 6.1. Limitations

There were several limitations for these two cases being proposed. The major limitation for the heat storage in the depleted SAGD pads, is having access to reservoir simulation model and steam monitoring to account for reasonable lifetime of the project and the duration steam can be stored and recovered without affecting the integrity of the reservoir.

The major limitation for the heat recovery for district heating is accounting for accurate amount of heat loss occurring in the geothermal wells, heat pumps, heat exchange stations and the underground geothermal pipes across the whole facility. By having more accurate estimation, the size of the facility and infrastructure needed can be designed more properly.

For both scenarios, the Alberta government's directives and regulations for decommissioned wells retrofitting either for heat storage or recovery needs to be revisited to make sure the designs being proposed are in line with the directives and there are no regulations against either of the cases.

### 6.2. Recommendations and Future Research

There could be lots of future research recommendations proposed for these two scenarios, few are highlighted as:

**Reservoir Simulation Model:** The reservoir engineering simulation model for the heat storage project in the depleted SAGD pads is quite important. The thermal storage capacity of the subsurface formations needs to be evaluated by having pore space, the heat capacity of the rock, thermal conductivity, and reservoir geometry. The permeability of the formation impact on hot fluid injectivity and heat recovery needs to be analyzed.

**Steam Degradation:** The steam degradation due to condensation to base and cap rock needs to be considered. This way project lifetime can be predicted more accurately. And the time duration steam can be stored and recovered when solar radiation not available.

**Parabolic Solar Trough Capacity:** In FIREBAG project it has been assumed the Solar trough capacity to be 80%. This is normally Capacity for desert climate most of the times cloud free, dust free. For FIREBAG location this might not be always the case, therefore steam storage duration and recovery factor becomes more important if solar trough capacity would be less.

**Surface Facility:** SAGD operations are designed for steam injection from the beginning. It was considered same facility and infrastructure to be used for geothermal steam injection and recovery. There might be some modifications to be applied and make this approach more practical.

**Cap Rock Integrity:** The cap rock integrity of the overburden formations can impact the duration of heat storage. The design factors required for steam injection and production, such as temperature and pressure should be analyzed thoroughly to avoid hydraulic fracturing or damaging the reservoir rock.

**Geothermal Wells Configuration and Spacing:** The geothermal wells spacing can play a big factor in the amount of heat can be transferred to the geothermal fluid. Therefore, it is a valid point to do sensitivity analysis of how this spacing would impact the geothermal district heating project, and modification in the number of the wells

**Water Temperature, Chemical and PH Changes:** In the Geothermal open loop, as the geothermal fluid circulates, the water temperature, chemical and PH changes throughout the process. The impact of these changes on the wells' casing, tubing, geothermal pipes, and the heat pumps needs to be studied to make sure the impact is not going to cause possible precipitation of harmful elements, resulting in corrosion to stop the operation.

**Integrating the two proposed projects:** The two separate location are proposed, FIREBAG for geothermal heat storage and Turner Valley for district heating application. It would be interesting to see if one location such as FIREBAG is used for both geothermal heat storage and district heating applications. The depleted SAGD pads temperature tends to remain high years post operation so this would be an advantage to utilize it for both heat storage and district heat recovery and study the impacts on GHG emissions and the economics.

## References


(2020). Retrieved from ihsmarkit: https://ihsmarkit.com/products/canada-well-header-data.html

Augustine, C. (2014). Analysis of Sedimentary Geothermal Systems Using an Analytical Reservoir Model. *GRC Transactions*, 641-648.

Bloomquist, D. R. (2012). *Geothermal Space Heating.* Washington State University Energy Program .

Budd, C. F. (1984, February 1). Geothermal Energy for Electrical Generation. Society of Petroleum Engineers. *Society of Petroleum Engineers*, 189-195.

Ghoreishi-Madiseh, S., Templeton, J., Hassani, F., Al-Khawja, M., & Aflaki, E. (2014). Geothermal Energy Extraction From Decommissioned Petroleum Wells. *Asian Rock Mechanism*, 2644-2653.

Gudmundsson, O., Thorsen, J., & Zhang, L. (2013). *Cost analysis of district heating compared to its competing technologies.* WIT Transactions on Ecology and The Environment.

Helmenstine, T. (2020, February 11). *Calculate Energy Required to Turn Ice Into Steam*. Retrieved from Thoghtco: thoughtco.com/ice-to-steam-energy-calculation-609497.

Hirschmiller, J. (2019, November). Retrieved from https://www.gljpc.com/blog/what-geothermal-energy-what-canada%E2%80%99s-potential

Hislop, J. (2018, February 19). Retrieved from Energi.media: https://energi.media/canada/canada-coal-natural-gas-power-regulations-19feb18/

Holman, J. P. (2009). Heat Transfer. In J. P. Holman, *Heat Transfer* (p. 752). McGraw-Hill Education.

J.M.K.C. Donev, e. a. (2018). *Energy Education - Steam assisted gravity drainage*. Retrieved from https://energyeducation.ca/encyclopedia/Steam_assisted_gravity_drainage

JACOS. (2018, February 28). Retrieved from www.aer.ca: https://www.aer.ca/documents/oilsands/insitu-presentations/2018AthabascaJACOSHangingstoneExpansionS.pdf

Kolker, A. H. (2005). Geothermal Potential Of Alaska. *American Rock Mechanics Association*.

Lee, S.-R. Y.-H.-B.-W. (2013). Evaluation of Heat Exchange Rate for Different Types of Ground Heat Exchangers. *International Society of Offshore and Polar Engineers.*

McTigue, J. C. (2018). “Hybridizing a geothermal power plant with concentrating solar power and thermal storage to increase power generation and dispatchability". *Applied Energy*.

Milkov, N., Danel, Q., Punov, P., Podevin, P., & Evtimov, T. (2017, November 7). *Experimental study on Rankine cycle evaporator efficiency intended for exhaust waste heat recovery of a diesel engine*. Retrieved from Matec Web Conferences: https://www.matec-conferences.org/articles/matecconf/abs/2017/47/matecconf_bultrans2017_04003/matecconf_bultrans2017_04003.html

Moazami, S. (2020). *Geologic Thermal Heat Storage and Recovery.* University of Calgary.

Nathan Schuknecht, J. M. (2018, November 8). *Achievement of the $100/m2 Parabolic trough.* Retrieved from https://aip.scitation.org/doi/pdf/10.1063/1.5067035

Nayef, M. (2013). Renewable Energy at Kuwait Great Burgan Oil Field. *Society of Petroleum Engineers*.

*Nesjavellir Geothermal Power Plant.* (2013). Retrieved from www.nat.is: https://www.nat.is/nesjavellir-geothermal-power-plant/

Omusi, D. (2019, April). *Optimal Energy Management of a SAGD Microgrid Participating in a Volatile*. Retrieved from https://prism.ucalgary.ca/bitstream/handle/1880/110265/ucalgary_2019_omusi_dominic.pdf?sequence=1

*Packer Plus*. (2020). Retrieved from https://packersplus.com/performance/custom-solution-saves-tight-gas-well-in-western-canada/

Quaschning, V. (2003, 6). *Solar thermal power plants.* Retrieved from Renewable Energy World: https://www.volker-quaschning.de/articles/fundamentals2/index_e.php

*R134a - Pressure Table*. (2008, January). Retrieved from NIST Chemistry WebBook: https://www.ohio.edu/mechanical/thermo/property_tables/R134a/R134a_PresSat.html

Reid, J. (2017). *Geothermal Heat in Calgary: An Oil and Gas Retrofit.* Calgary: University of Calgary.

*Residential Electricity and Natural Gas Plans*. (2014). Retrieved from energyrates.ca: https://energyrates.ca/residential-electricity-natural-gas/

*RetScreen*. (2020).

SMU. (2020). *SMU Geothermal Lab*. Retrieved from Heat Flow and Heat Loss: https://www.smu.edu/Dedman/Academics/Departments/Earth-Sciences/Research/GeothermalLab/LabResearch/HeatFlowandHeatLoss

Soucy, P. (2014, November 4). *Paarbolic Solar Trough*. Retrieved from https://www.parabolicsolartrough.com/

Urieli, I. (2020). *Refrigerant and Heat Pumps.* Retrieved from https://www.ohio.edu/mechanical/thermo/intro/chapt.1_6/chapter4c.html

*Water Specific Heat.* (2020). Retrieved from https://www.engineeringtoolbox.com/specific-heat-capacity-water-d_660.html

Wendt, e. a. (2019). Geologic Thermal Energy Storage of Solar Heat to Provide a Source of Dispatchable Renewable Power and Seasonal Energy Storage Capacity. *GRC Transactions*, 73-91.

Wilson, N. (2016). Alberta Government Eyes Geothermal Fix to Abandoned Well Crisis. *Alberta Oil Magazine*.

Xu, E. J. (2018, June). *Green Energy Island Integration and Operation Optimization Research*. Retrieved from https://www.researchgate.net/figure/a-b-c-Schematic-and-T-s-diagram-for-the-ideal-vapor-compression-refrigeration-cycle_fig2_326912104

Zipp, K. (2012, May 2). *World's Largest Aperture Parabolic Trough Installation.* Retrieved from Solar Power World: https://www.solarpowerworldonline.com/2012/05/worlds-largest-aperture-parabolic-trough-installation/

# Appendix A: Geothermal Heat Energy Storage (GeoTES) Numerical Model

Design for Solar Trough Field
Number of Parabolic Troughs Needed

| Month | Earth Temp | Daily Solar Radiation Power | Atmospheric Pressure | Average Electricity consumption per household a month | Average Electricity consumption for 1000 household a month | Average Electricty Household per day | Average Electricity for 1000 household per day | Input Steam Energy to Turbine | Input Steam Energy to Turbine for 1000 Household | Input Steam to Vaporizer | Input Steam to Vaporizer for 1000 Households | Output from Solar Trough | Output from Solar Trough for 1000 Households | Capacity 80% | m2 Solar Trough field for 1000 Households | Number of Solar Trough if each 50 m2 |
|---|---|---|---|---|---|---|---|---|---|---|---|---|---|---|---|---|
| | C° | $kWh/m^2/d$ | kPa | kWh | kWh | kWh/day | kWh/day | kWh/day | kWh/day | kWh/day | kWh/day | kWh/day | kWh/day | kWh/day | m2 Area | Number of Trough |
| January | -9.6 | 1.58 | 100.9 | 800 | 800000 | 26.67 | 26666.67 | 76.2 | 76190.49 | 152.4 | 152380.98 | 203.2 | 203174.64 | 253968.3 | 160739.4304 | 3214.788608 |
| February | -7.8 | 2.53 | 100.9 | 800 | 800000 | 26.67 | 26666.67 | 76.2 | 76190.49 | 152.4 | 152380.98 | 203.2 | 203174.64 | 253968.3 | 100382.7273 | 2007.654545 |
| March | -2.3 | 3.62 | 100.9 | 800 | 800000 | 26.67 | 26666.67 | 76.2 | 76190.49 | 152.4 | 152380.98 | 203.2 | 203174.64 | 253968.3 | 70156.98895 | 1403.139779 |
| April | 5.6 | 4.46 | 100.7 | 500 | 500000 | 16.67 | 16666.67 | 47.63 | 47619.06 | 95.26 | 95238.12 | 127.0133333 | 126984.16 | 158730.2 | 35589.73094 | 711.7946188 |
| May | 13.4 | 5.1 | 100.7 | 400 | 400000 | 13.33 | 13333.33 | 38.09 | 38095.23 | 76.18 | 76190.46 | 101.5733333 | 101587.28 | 126984.1 | 24898.84314 | 497.9768627 |
| June | 18.9 | 5.61 | 100.5 | 400 | 400000 | 13.33 | 13333.33 | 38.09 | 38095.23 | 76.18 | 76190.46 | 101.5733333 | 101587.28 | 126984.1 | 22635.31194 | 452.7062389 |
| July | 20.5 | 5.52 | 100.6 | 400 | 400000 | 13.33 | 13333.33 | 38.09 | 38095.23 | 76.18 | 76190.46 | 101.5733333 | 101587.28 | 126984.1 | 23004.36594 | 460.0873188 |
| August | 19.5 | 4.91 | 100.7 | 400 | 400000 | 13.33 | 13333.33 | 38.09 | 38095.23 | 76.18 | 76190.46 | 101.5733333 | 101587.28 | 126984.1 | 25862.34216 | 517.2468432 |
| September | 15.1 | 3.77 | 100.9 | 400 | 400000 | 13.33 | 13333.33 | 38.09 | 38095.23 | 76.18 | 76190.46 | 101.5733333 | 101587.28 | 126984.1 | 33682.78515 | 673.6557029 |
| October | 8.3 | 2.38 | 100.9 | 500 | 500000 | 16.67 | 16666.67 | 47.63 | 47619.06 | 95.26 | 95238.12 | 127.0133333 | 126984.16 | 158730.2 | 66693.36134 | 1333.867227 |
| November | 2.1 | 1.45 | 100.9 | 800 | 800000 | 26.67 | 26666.67 | 76.2 | 76190.49 | 152.4 | 152380.98 | 203.2 | 203174.64 | 253968.3 | 175150.5517 | 3503.011034 |
| December | -4.5 | 1.28 | 100.9 | 800 | 800000 | 26.67 | 26666.67 | 76.2 | 76190.49 | 152.4 | 152380.98 | 203.2 | 203174.64 | 253968.3 | 198412.7344 | 3968.254688 |
| | | | | | 7000000 | | 233333.33 | | 666666.66 | | 1333333.32 | | 1777777.76 | 2222222.2 | | 4000 Solar troughs for Daytime need |

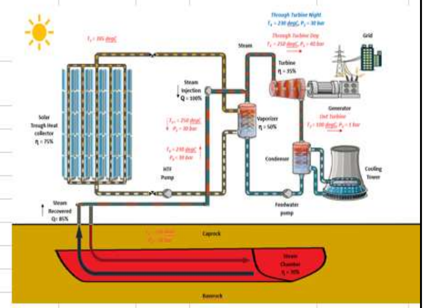


Design for Steam to be injected
Number of Pads and rate needed

CWE

| Month | Earth Temp | Daily Solar Radiation Power | Atmospheric Pressure | Average Electricity consumption per household a month | Average Electricity consumption for 1000 household a month | Average Electricty for 1000 household per day | Input Steam Energy to Turbine for 1000 Household | Input Steam Mass to Turbine for 1000 Households Ti = 250 C, Pi=40Bar Enti = 0.778 kWh/kg To = 100C Po=1 bar Ento= 0.743 kWh/kg | Output Steam Energy from GeoTES for 1000 Household 6hour | Output Steam Energy from GeoTES for 1000 Household 6hour, efficiency 70% | Output Steam Mass from GeoTES for 1000 Households for 6hour Ti = 250 C, Pi=40Bar Enti= 0.778 kWh/kg To = 100C Po=1 bar | Steam Mass quality of vapor 85% | Input CWE (Cold Water Equvalent) volume density = 1000 kg/m3 | Inject volume CWE (Cold Water Equvalent) per hour | Inject volume CWE (Cold Water Equvalent) per day | Inject volume CWE (Cold Water Equvalent) per day with rate 300m3/day |
|---|---|---|---|---|---|---|---|---|---|---|---|---|---|---|---|---|
| | C° | $kWh/m^2/d$ | kPa | kWh | kWh | kWh/day | kWh/day | kg/day | kWh/ 6hour | kWh/ 6hour | kg/6hour | kg/6hr | m3/6hr | m3/hr | m3/day | |
| January | -9.6 | 1.58 | 100.9 | 800 | 800000 | 26666.67 | 76190.49 | 2176871.14 | 19047.62 | 27210.89 | 777454 | 914651.76 | 914.65 | 152.44 | 3658.61 | 12.2 |
| February | -7.8 | 2.53 | 100.9 | 800 | 800000 | 26666.67 | 76190.49 | 2176871.14 | 19047.62 | 27210.89 | 777454 | 914651.76 | 914.65 | 152.44 | 3658.61 | 12.2 |
| March | -2.3 | 3.62 | 100.9 | 800 | 800000 | 26666.67 | 76190.49 | 2176871.14 | 19047.62 | 27210.89 | 777454 | 914651.76 | 914.65 | 152.44 | 3658.61 | 12.2 |
| April | 5.6 | 4.46 | 100.7 | 500 | 500000 | 16666.67 | 47619.06 | 1360544.57 | 11904.77 | 17006.81 | 485908.86 | 571657.48 | 571.66 | 95.28 | 2286.63 | 7.62 |
| May | 13.4 | 5.1 | 100.7 | 400 | 400000 | 13333.33 | 38095.23 | 1088435.14 | 9523.81 | 13605.44 | 388726.86 | 457325.72 | 457.33 | 76.22 | 1829.30 | 6.1 |
| June | 18.9 | 5.61 | 100.5 | 400 | 400000 | 13333.33 | 38095.23 | 1088435.14 | 9523.81 | 13605.44 | 388726.86 | 457325.72 | 457.33 | 76.22 | 1829.30 | 6.1 |
| July | 20.5 | 5.52 | 100.6 | 400 | 400000 | 13333.33 | 38095.23 | 1088435.14 | 9523.81 | 13605.44 | 388726.86 | 457325.72 | 457.33 | 76.22 | 1829.30 | 6.1 |
| August | 19.5 | 4.91 | 100.7 | 400 | 400000 | 13333.33 | 38095.23 | 1088435.14 | 9523.81 | 13605.44 | 388726.86 | 457325.72 | 457.33 | 76.22 | 1829.30 | 6.1 |
| September | 15.1 | 3.77 | 100.9 | 400 | 400000 | 13333.33 | 38095.23 | 1088435.14 | 9523.81 | 13605.44 | 388726.86 | 457325.72 | 457.33 | 76.22 | 1829.30 | 6.1 |
| October | 8.3 | 2.38 | 100.9 | 500 | 500000 | 16666.67 | 47619.06 | 1360544.57 | 11904.77 | 17006.81 | 485908.86 | 571657.48 | 571.66 | 95.28 | 2286.63 | 7.62 |
| November | 2.1 | 1.45 | 100.9 | 800 | 800000 | 26666.67 | 76190.49 | 2176871.14 | 19047.62 | 27210.89 | 777454 | 914651.76 | 914.65 | 152.44 | 3658.61 | 12.2 |
| December | -4.5 | 1.28 | 100.9 | 800 | 800000 | 26666.67 | 76190.49 | 2176871.14 | 19047.62 | 27210.89 | 777454 | 914651.76 | 914.65 | 152.44 | 3658.61 | 12.2 |
| | | | | 7000 | | | | | | | | | | | | 12 Pair needed |

## Appendix B: Geothermal Space Heating Numerical Model

| Calgary Average House | Volume with 9ft Ceiling | Volume | Air Density | Air Mass in the house | Air Mass needed | Vent to replace 70% in an hour | Mass Flow Rate replaced in a second | Heat Energy | Heat Power | Qout/Mass = (H2-H3) | Mass Flow Rate of Refrigerant, Mass = Qout/H2-H3) | $W_{in}$ , Mass*(H2-H1) | Qin = Mass* (H1-H4) | Qin = Mass *(Specific Heat difference water at 40 and 26.7 degC) | Mass Rate | Water Density 1000 kg/m3 Volume flow rate | For 1000 Households | Water Density 1000 kg/m3 Volume flow rate needed for 1000 households | Water Density 1000 kg/m3 Volume flow rate needed for 1000 households a day | Speed of flow |
|---|---|---|---|---|---|---|---|---|---|---|---|---|---|---|---|---|---|---|---|---|
| ft2 | ft3 | m3 | kg/m3 | kg | kg | kg/hour | kg/s | kJ/hour | kW | kJ/kg | kg/s | kW | kW | kW | kg/s | m3/s | kg/s | m3/s | m3 | m/s |
| 2000 | 18000 | 509.4 | 1.2754 | 649.68876 | 650 | 455 | 0.126389 | 4572.75 | 1.270208 | 182.2 | 0.006971506 | 0.20844802 | 1.06176 | 1.061760314 | 0.019083 | 1.90827E-05 | 19.08267997 | 0.01908268 | 1648.74355 | 0.002093 |
| | | | | | | | | | | | | | | | | | | 68.69764791 | | |
| Average Temp | 15 degC | | | | | | | | | | | | | | | | | 1648.74355 | | |
| Desired Temp | 25 degC | | | | | | | | | | | | | | | | | | | |
| Specific Heat of Air At 300K | 1.005 kJ/kg.K | | | | | | | | | | | | | | | | | | | |
| q = Mass Flow rate * Specific Heat Air * Temp difference | | | | | | | | | | | | | | | | | | | | |
| Heat pump rate of the heat output | 5.08 kW | | | | | | | | | | | | | | | | | | | |
| Using Refrigerant R134a | | H1 = 241.1kJ/kg @ 1.6bar | H2 = 271kJ/kg @10bar | H4 = 88.8kJ/kg @ 26.7 degC | S1= S2 = 0.942kJ/kg.K @1.63bar | S3 = 0.3324 kJ/kg.K @ 26.7 degc | S4 = 0.127 kJ/kg.K @ 1.6bar | | | Evaporator: $t_{in}$= 40 degc $t_{out}$= 26.7 degc | Specific Heat water = 4.186J/g.C $SP_{in}$= 167.4 J/g $SP_{out}$= 111.76 J/g | Specific Heat water = 4.186J/g.C $SP_{in}$= 167.4 J/g or kJ/kg $SP_{out}$= 111.76 J/g or kJ/kg | | Tubing 88.9mm 0.0889m | BH Size 222mm | Casing Size 139.7mm 0.1397m | Borehole depth 2000m | Casing Volume | Tubing volume | |
| | | | | | | | | | | | | | | | | | | m3 | m3 | |
| | | | | | | | | | | | | | | | | | | 30.6402613 | 12.4080397 | |
| | | | | | | | | | | | | | | | | | | Casing Area | Tubing Section Area | Circulation Area |
| | | | | | | | | | | | | | | | | | | m2 | m2 | m2 |
| | | | | | | | | | | | | | | | | | | 0.015320131 | 0.00620402 | 0.009116 |

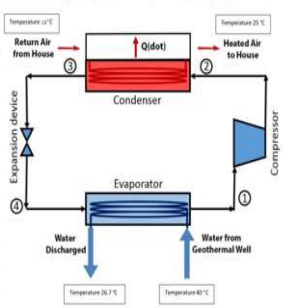


Evaporator: Low P Liquid to low P Vapor by Absorbing heat
Compressor: low P, Low Temp Vapor to High P and High Temp Vapor
Condenser: high P Vapor to high P liquid
Expansion Valve: high P liquid to low P liquid

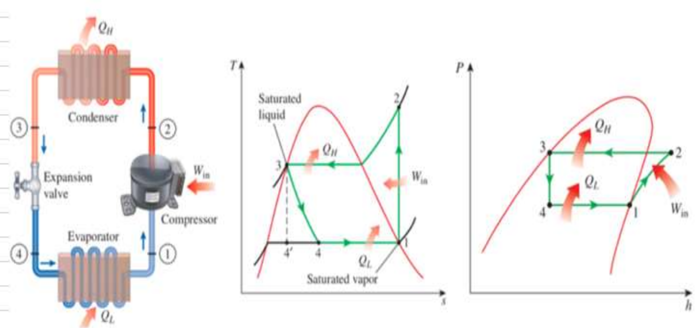


Cond: P same, T down
Eva: P same, T up

## Appendix C: Geothermal Well Numerical Model

| Bottom Hole Temp | Surface Temp | Total Depth | BS Diameter | BS Radius | Casing Diameter | Casing Radius | Tubing Diameter | Tubing Radius | Each well Input Mass Flow rate | | Length | Area (Outside - inside Area) | Each Well Output Mass Flow rate |
|---|---|---|---|---|---|---|---|---|---|---|---|---|---|
| $T_{BH}$ | $T_S$ | H | BS | $R_{BS}$ | CS | $R_{CS}$ | T | $R_T$ | $m'_i$ | Cp | Length | | $m'_o$ |
| degC | degC | m | m | m | m | m | m | m | kg/s | J/kg.K | m | m2 | kg/s |
| 55 | 5 | 2000 | 0.2 | 0.1 | 0.1397 | 0.06985 | 0.0889 | 0.04445 | 5 | 4181 | 2000 | 0.0062 | 10 |

| | | diameter | radius | | |
|---|---|---|---|---|---|
| | in | cm | cm | cm | m |
| BS | 7.87 | 19.9898 | 9.9949 | 8.48995 | 0.0849 |
| CS | 5.5 | 13.97 | 6.985 | | |
| TB | 3.5 | 8.89 | 4.445 | | |

$c = 3E\text{-}5*(Temp)^2 - 0.0023*(Temp) + 4.2186$

$\rho = -0.0041*(Temp)^2 - 0.0324*(Temp) + 999.93$

$\mu = 3.31E\text{-}7*(Temp)^2 - 4.07E\text{-}5*(Temp) + 1.72E\text{-}3$

$k = -9.93E\text{-}7*(Temp)^2 + 2.08E\text{-}3*(Temp) + 5.66E\text{-}1$

$Pr = 0.0027*(Temp)^2 - 0.3257*(Temp) + 12.717$

$Q' = 2\pi\, r\, h(T\infty - Ti)\, \Delta z$

sn

$Nu = 0.023*Re^{0.8}*Pr^{0.4}$

$h = Nu*k/Dh$

$Q' = m'*(c*(Tco - Tci))$

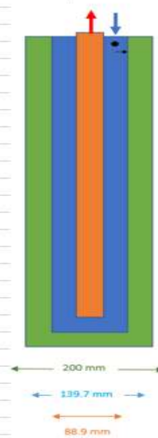


| | | Temp Dependant | | | | | | | | | | | | | | |
|---|---|---|---|---|---|---|---|---|---|---|---|---|---|---|---|---|
| z | Temp | c | ρ | μ | k | Pr | $D_h$ Do-Di | Re | Nu | h | Q' | T2 | Q' | Volume Rate | Speed | Time |
| m | DegC | kJ/kg.C | | | W/m.K | | | | | W/m$^2$.K | W | degC | kW | m3/s | m/s | h |
| 0 | 5 | 4.207352 | 999.6655 | 0.001525 | 0.576152 | 11.156 | 0.1111 | 14459.29 | 128.4839 | 666.3029 | | 26.7 | | 0.010003 | 1.613443 | 0 |
| 10 | 5.25 | 4.206858 | 999.6469 | 0.001515 | 0.576646 | 11.08149 | 0.1111 | 14548.28 | 128.7705 | 668.3624 | -77128.775 | 24.866594 | -77.12878 | 0.010004 | 1.613473 | 0.001722 |
| 20 | 5.5 | 4.206367 | 999.6278 | 0.001506 | 0.57714 | 11.00733 | 0.1111 | 14637.97 | 129.0581 | 670.4279 | -69939.189 | 23.203896 | -69.93919 | 0.010004 | 1.613504 | 0.003443 |
| 30 | 5.75 | 4.20588 | 999.6081 | 0.001497 | 0.577632 | 10.93349 | 0.1111 | 14728.37 | 129.3466 | 672.4996 | -63314.903 | 21.698506 | -63.3149 | 0.010004 | 1.613535 | 0.005165 |
| 40 | 6 | 4.205397 | 999.588 | 0.001488 | 0.578123 | 10.86 | 0.1111 | 14819.47 | 129.6361 | 674.5774 | -57213.306 | 20.338032 | -57.21331 | 0.010004 | 1.613568 | 0.006886 |
| 50 | 6.25 | 4.204918 | 999.5673 | 0.001479 | 0.578612 | 10.78684 | 0.1111 | 14911.3 | 129.9266 | 676.6614 | -51594.851 | 19.11102 | -51.59485 | 0.010004 | 1.613601 | 0.008607 |
| 60 | 6.5 | 4.204442 | 999.5462 | 0.001469 | 0.5791 | 10.71403 | 0.1111 | 15003.84 | 130.218 | 678.7514 | -46422.85 | 18.006882 | -46.42285 | 0.010005 | 1.613636 | 0.010329 |
| 70 | 6.75 | 4.20397 | 999.5245 | 0.00146 | 0.579588 | 10.64154 | 0.1111 | 15097.12 | 130.5103 | 680.8476 | -41663.275 | 17.015836 | -41.66327 | 0.010005 | 1.613671 | 0.01205 |
| 80 | 7 | 4.203502 | 999.5023 | 0.001451 | 0.580073 | 10.5694 | 0.1111 | 15191.12 | 130.8037 | 682.9499 | -37284.577 | 16.128847 | -37.28458 | 0.010005 | 1.613706 | 0.013771 |
| 90 | 7.25 | 4.203038 | 999.4796 | 0.001442 | 0.580558 | 10.49759 | 0.1111 | 15285.87 | 131.098 | 685.0583 | -33257.513 | 15.337574 | -33.25751 | 0.010005 | 1.613743 | 0.015492 |
| 100 | 7.5 | 4.202577 | 999.4564 | 0.001433 | 0.581041 | 10.42613 | 0.1111 | 15381.36 | 131.3932 | 687.1728 | -29554.988 | 14.634315 | -29.55499 | 0.010005 | 1.613781 | 0.017213 |
| 110 | 7.75 | 4.20212 | 999.4326 | 0.001424 | 0.581524 | 10.35499 | 0.1111 | 15477.61 | 131.6894 | 689.2934 | -26151.901 | 14.011965 | -26.1519 | 0.010006 | 1.613819 | 0.018934 |
| 120 | 8 | 4.201667 | 999.4084 | 0.001416 | 0.582004 | 10.2842 | 0.1111 | 15574.61 | 131.9866 | 691.4202 | -23025.008 | 13.463968 | -23.02501 | 0.010006 | 1.613858 | 0.020654 |
| 130 | 8.25 | 4.196522 | 999.3836 | 0.001407 | 0.582484 | 10.21374 | 0.1111 | 15672.37 | 132.2847 | 693.553 | -20152.791 | 12.983742 | -20.15279 | 0.010006 | 1.613898 | 0.022375 |
| 140 | 8.5 | 4.196118 | 999.3584 | 0.001398 | 0.582963 | 10.14363 | 0.1111 | 15770.9 | 132.5838 | 695.692 | -17513.351 | 12.566372 | -17.51335 | 0.010006 | 1.613939 | 0.024096 |
| 150 | 8.75 | 4.195717 | 999.3326 | 0.001389 | 0.58344 | 10.07384 | 0.1111 | 15870.21 | 132.8838 | 697.837 | -15090.689 | 12.206703 | -15.09069 | 0.010007 | 1.61398 | 0.025816 |
| 160 | 9 | 4.19532 | 999.3063 | 0.001381 | 0.583916 | 10.0044 | 0.1111 | 15970.29 | 133.1848 | 699.9881 | -12867.704 | 11.899987 | -12.8677 | 0.010007 | 1.614023 | 0.027536 |
| 170 | 9.25 | 4.194927 | 999.2795 | 0.001372 | 0.58439 | 9.935294 | 0.1111 | 16071.17 | 133.4867 | 702.1453 | -10828.586 | 11.641852 | -10.82859 | 0.010007 | 1.614066 | 0.029257 |
| 180 | 9.5 | 4.194538 | 999.2522 | 0.001363 | 0.584864 | 9.866525 | 0.1111 | 16172.83 | 133.7896 | 704.3086 | -8958.7273 | 11.428271 | -8.958727 | 0.010007 | 1.61411 | 0.030977 |
| 190 | 9.75 | 4.194152 | 999.2243 | 0.001355 | 0.585336 | 9.798094 | 0.1111 | 16275.29 | 134.0934 | 706.478 | -7244.6283 | 11.255539 | -7.244628 | 0.010008 | 1.614155 | 0.032697 |
| 200 | 10 | 4.19377 | 999.196 | 0.001346 | 0.585807 | 9.73 | 0.1111 | 16378.55 | 134.3982 | 708.6534 | -5673.8229 | 11.120248 | -5.673823 | 0.010008 | 1.614201 | 0.034417 |
| 210 | 10.25 | 4.193392 | 999.1671 | 0.001338 | 0.586277 | 9.662244 | 0.1111 | 16482.62 | 134.7039 | 710.8348 | -4234.8005 | 11.01926 | -4.2348 | 0.010008 | 1.614248 | 0.036137 |
| 220 | 10.5 | 4.193018 | 999.1378 | 0.001329 | 0.586745 | 9.594825 | 0.1111 | 16587.51 | 135.0105 | 713.0223 | -2916.9368 | 10.949694 | -2.916937 | 0.010009 | 1.614295 | 0.037856 |
| 230 | 10.75 | 4.192647 | 999.1079 | 0.001321 | 0.587212 | 9.527744 | 0.1111 | 16693.22 | 135.3181 | 715.2158 | -1710.4288 | 10.908898 | -1.710429 | 0.010009 | 1.614343 | 0.039576 |
| 240 | 11 | 4.19228 | 999.0775 | 0.001312 | 0.587678 | 9.461 | 0.1111 | 16799.75 | 135.6266 | 717.4153 | -606.23381 | 10.894437 | -0.606234 | 0.010009 | 1.614393 | 0.041295 |
| 250 | 11.25 | 4.191917 | 999.0466 | 0.001304 | 0.588143 | 9.394594 | 0.1111 | 16907.11 | 135.936 | 719.6207 | 403.98638 | 10.904074 | 0.4039864 | 0.01001 | 1.614442 | 0.043015 |
| 260 | 11.5 | 4.191558 | 999.0152 | 0.001296 | 0.588607 | 9.328525 | 0.1111 | 17015.32 | 136.2464 | 721.8322 | 1327.9183 | 10.935755 | 1.3279183 | 0.01001 | 1.614493 | 0.044734 |
| 270 | 11.75 | 4.191202 | 998.9832 | 0.001287 | 0.589069 | 9.262794 | 0.1111 | 17124.36 | 136.5577 | 724.0496 | 2172.64523 | 10.987593 | 2.1726452 | 0.01001 | 1.614545 | 0.046453 |
| 280 | 12 | 4.19085 | 998.9508 | 0.001279 | 0.58953 | 9.1974 | 0.1111 | 17234.26 | 136.8699 | 726.273 | 2944.6925 | 11.057858 | 2.9446925 | 0.010011 | 1.614597 | 0.048172 |
| 290 | 12.25 | 4.190502 | 998.9178 | 0.001271 | 0.58999 | 9.132344 | 0.1111 | 17345.01 | 137.183 | 728.5022 | 3650.06947 | 11.144962 | 3.6500695 | 0.010011 | 1.614651 | 0.04989 |
| 300 | 12.5 | 4.190158 | 998.8844 | 0.001263 | 0.590448 | 9.067625 | 0.1111 | 17456.62 | 137.4971 | 730.7374 | 4294.30851 | 11.247447 | 4.2943085 | 0.010011 | 1.614705 | 0.051609 |
| 310 | 12.75 | 4.189817 | 998.8504 | 0.001255 | 0.590906 | 9.003244 | 0.1111 | 17569.1 | 137.812 | 732.9784 | 4882.50122 | 11.36398 | 4.8825012 | 0.010012 | 1.61476 | 0.053328 |
| 320 | 13 | 4.18948 | 998.8159 | 0.001247 | 0.591362 | 8.9392 | 0.1111 | 17682.45 | 138.1278 | 735.2253 | 5419.332 | 11.493336 | 5.419332 | 0.010012 | 1.614815 | 0.055046 |
| 330 | 13.25 | 4.189147 | 998.7809 | 0.001239 | 0.591817 | 8.875494 | 0.1111 | 17796.68 | 138.4446 | 737.4781 | 5909.10918 | 11.634393 | 5.9091092 | 0.010012 | 1.614872 | 0.056764 |
| 340 | 13.5 | 4.188818 | 998.7454 | 0.001231 | 0.59227 | 8.812125 | 0.1111 | 17911.79 | 138.7622 | 739.7366 | 6355.79394 | 11.786126 | 6.3557939 | 0.010013 | 1.614929 | 0.058482 |
| 350 | 13.75 | 4.188492 | 998.7093 | 0.001223 | 0.592723 | 8.749094 | 0.1111 | 18027.79 | 139.0807 | 742.0009 | 6763.02704 | 11.947592 | 6.763027 | 0.010013 | 1.614988 | 0.0602 |
| 360 | 14 | 4.18817 | 998.6728 | 0.001215 | 0.593174 | 8.6864 | 0.1111 | 18144.68 | 139.4002 | 744.271 | 7134.15364 | 12.117933 | 7.1341536 | 0.010013 | 1.615047 | 0.061918 |
| 370 | 14.25 | 4.187852 | 998.6357 | 0.001207 | 0.593624 | 8.624044 | 0.1111 | 18262.48 | 139.7204 | 746.5468 | 7472.24629 | 12.29636 | 7.4722463 | 0.010014 | 1.615107 | 0.063635 |
| 380 | 14.5 | 4.187538 | 998.5982 | 0.001199 | 0.594072 | 8.562025 | 0.1111 | 18381.18 | 140.0416 | 748.8283 | 7780.12617 | 12.482152 | 7.7801262 | 0.010014 | 1.615167 | 0.065353 |
| 390 | 14.75 | 4.187227 | 998.5601 | 0.001192 | 0.59452 | 8.500344 | 0.1111 | 18500.79 | 140.3636 | 751.1154 | 8060.3828 | 12.674651 | 8.0603828 | 0.010014 | 1.615229 | 0.06707 |
| 400 | 15 | 4.18692 | 998.5215 | 0.001184 | 0.594966 | 8.439 | 0.1111 | 18621.31 | 140.6865 | 753.4082 | 8315.3923 | 12.873255 | 8.3153923 | 0.010015 | 1.615291 | 0.068787 |
| 410 | 15.25 | 4.186617 | 998.4824 | 0.001176 | 0.595411 | 8.377994 | 0.1111 | 18742.76 | 141.0102 | 755.7066 | 8547.33417 | 13.077414 | 8.5473342 | 0.010015 | 1.615355 | 0.070504 |
| 420 | 15.5 | 4.186318 | 998.4428 | 0.001169 | 0.595854 | 8.317325 | 0.1111 | 18865.13 | 141.3348 | 758.0105 | 8758.20695 | 13.286624 | 8.7582069 | 0.010016 | 1.615419 | 0.072221 |
| 430 | 15.75 | 4.186022 | 998.4026 | 0.001161 | 0.596297 | 8.256994 | 0.1111 | 18988.44 | 141.6603 | 760.32 | 8949.84256 | 13.500427 | 8.9498426 | 0.010016 | 1.615484 | 0.073937 |
| 440 | 16 | 4.18573 | 998.362 | 0.001154 | 0.596738 | 8.197 | 0.1111 | 19112.68 | 141.9865 | 762.635 | 9123.91968 | 13.718404 | 9.1239197 | 0.010016 | 1.615549 | 0.075654 |
| 450 | 16.25 | 4.185442 | 998.3208 | 0.001146 | 0.597178 | 8.137344 | 0.1111 | 19237.87 | 142.3136 | 764.9554 | 9281.976 | 13.940172 | 9.281976 | 0.010017 | 1.615616 | 0.07737 |
| 460 | 16.5 | 4.185158 | 998.2792 | 0.001139 | 0.597617 | 8.078025 | 0.1111 | 19364 | 142.6415 | 767.2812 | 9425.41959 | 14.165383 | 9.4254196 | 0.010017 | 1.615684 | 0.079086 |
| 470 | 16.75 | 4.184877 | 998.237 | 0.001131 | 0.598054 | 8.019044 | 0.1111 | 19491.08 | 142.9702 | 769.6123 | 9555.53939 | 14.393718 | 9.5555394 | 0.010018 | 1.615752 | 0.080802 |
| 480 | 17 | 4.1846 | 998.1943 | 0.001124 | 0.59849 | 7.9604 | 0.1111 | 19619.12 | 143.2998 | 771.9488 | 9673.51488 | 14.624887 | 9.6735149 | 0.010018 | 1.615821 | 0.082517 |